East European Journal of Physics. 3. 20–43 (2026)
DOI: 10.26565/2312-4334-2026-3-03 ISSN 2312-4334

EXACT TRAVELING WAVES AND BIFURCATION STRUCTURE OF A COUPLED KUDRYASHOV-TYPE NONLINEAR SCHRÖDINGER SYSTEM VIA THE MODIFIED EXTENDED MAPPING METHOD

Wafy M. Hasan[1,2], Hamdy M. Ahmed[3,*], Ahmed M. Ahmed[1], Haytham M. Rezk[1], Wafaa B. Rabie[4,5]
[1]*Department of Mathematics, Faculty of Science, Al-Azhar University, Cairo, Egypt*
[2]*Department of Basic Sciences, Faculty of Engineering Technology, ElSewedy University of Technology, Cairo, Egypt*
[3]*Department of Physics and Engineering Mathematics, Higher Institute of Engineering, El Shorouk Academy, Cairo, Egypt*
[4]*Department of Mathematics, Faculty of Science, Luxor University, Taiba Luxor, Egypt*
[5]*Luxor National University, Faculty of Computing, Information Technology, and Artificial Intelligence, Luxor, Egypt*
[*]*Corresponding Author e-mail: hamdy_17eg@yahoo.com*
Received May 15, 2026; revised June 20, 2026; accepted July 6, 2026

This study obtains exact traveling wave solutions and conducts a bifurcation analysis for the coupled (1+1)-dimensional Kudryashov's equation. This system of nonlinear Schrödinger-type equations models the simultaneous propagation of optical pulses in a birefringent fiber, incorporating critical higher-order effects like cubic-quartic dispersion and nonlinearities for enhanced physical accuracy. By applying the modified extended mapping method (MEMM), the coupled partial differential equations are systematically reduced to a manageable ordinary differential equation. This reduction allows for the construction of a broad spectrum of exact solutions such as bright and dark solitons, periodic waves, periodic singular solutions, along with singular solitons, in addition to hyperbolic, exponential, rational, and Weierstrass elliptic function solutions. A key component of the work is a detailed bifurcation analysis of the resulting planar dynamical system. This analysis identifies critical parameter thresholds and classifies all possible qualitative behaviors of the wave solutions, mapping out regions of existence for different solution types. The physical implications of both the derived solutions and the bifurcation structure are discussed in the context of nonlinear optics, particularly for pulse dynamics and stability in dual-polarization optical communication systems. The results demonstrate the efficacy of MEMM and provide new insights that contribute to the understanding and design of advanced optical waveguides.

Keywords: *Nonlinear Schrödinger equations; Birefringent optical fibers; Higher-order dispersion; Modified extended mapping method (MEMM); Exact traveling wave solutions; Bifurcation analysis*

1. INTRODUCTION

Partial differential equations (PDEs) serve as cornerstone mathematical models in numerous scientific and engineering fields, enabling the description of phenomena that evolve in both space and time. They are especially vital for capturing wave propagation, fluid flow, and other processes in which nonlinearity generates intricate structures such as shocks, turbulent states, and solitary waves. For example, the nonlinear Navier–Stokes model remains the principal instrument for examining intricate fluid dynamics, encompassing turbulence, vortex generation, and wave-breaking phenomena [1, 2]. Similarly, the Korteweg–de Vries model has occupied a pivotal position in clarifying the characteristics of nonlinear wave evolution and the appearance of solitons in shallow-water environments [3, 4]. The utility of PDEs extends far beyond classical physics: in environmental and geophysical contexts, they are routinely employed to model atmospheric and oceanic wave dynamics, while nonlinear advection–diffusion equations are used to track pollutant transport in air and water bodies [5, 6]. Engineering disciplines also rely heavily on PDEs for studying shock-wave phenomena, optical pulse evolution in fibers [7, 8], climate variability, and extreme meteorological events [9, 10]. The extraordinary breadth of these applications highlights the indispensable role of PDEs in tackling real-world problems across diverse domains.

Exact solutions to nonlinear evolution equations (NLEEs) can be constructed through a rich array of analytical techniques. Notable examples include the extended sinh–Gordon equation expansion method, which exploits known solutions of the sinh–Gordon equation to generate new solutions for wider classes of NLEEs [11]; the modified extended tanh-function method, which enhances the classical tanh expansion to yield richer solution families [12]; the modified extended direct algebraic approach, offering a structured framework that converts complex NLEEs into solvable algebraic systems [13, 14]; and the modified extended mapping method, which establishes versatile functional mappings to interconnect different solution types and thereby broaden the scope of treatable equations [15, 16]. Additional powerful tools encompass the modified Sardar sub-equation technique [17], the extended F-expansion method [18, 19], the improved modified extended tanh-function scheme [20, 21], the extended simplest equation method [22], Riccati–Bernoulli and Bäcklund Methods [23], among others. Taken together, these approaches offer vital tools for investigating advanced physical processes—such as wave propagation, fluid instabilities, and heat transfer phenomena—while linking rigorous theoretical advances with practical implementations across mathematical, physical, and engineering disciplines. The study

Cite as: W.M. Hasan, H.M. Ahmed, A.M. Ahmed, H.M. Rezk, W.B. Rabie, East Eur. J. Phys. 3, 20 (2026), https://doi.org/10.26565/2312-4334-2026-3-03

© W.M. Hasan, H.M. Ahmed, A.M. Ahmed, H.M. Rezk, W.B. Rabie, 2026; CC BY 4.0 license

of coupled nonlinear evolution equations (NLEEs) within optical settings continues to be an important research domain owing to their capacity to represent intricate wave interactions in birefringent fibers. Motivated by the need to uncover richer dynamical behaviors and transition mechanisms in such highly nonlinear systems—beyond what traditional solution methods reveal—this study focuses on deriving exact traveling wave solutions and performing a comprehensive bifurcation analysis for the coupled system of nonlinear Schrödinger equations with cubic-quartic dispersions and higher-order nonlinearities [24], given by

$$\begin{aligned}&iu_t + ia_1u_{xxx} + a_2u_{xxxx} + \frac{a_3u}{\alpha_1|u|^6 + \alpha_2|u|^4|v|^2 + \alpha_3|u|^2|v|^4 + \alpha_4|v|^6} + \frac{a_4u}{\left(\beta_1|u|^2 + \beta_2|v|^2\right)\sqrt{|u|^2 + |v|^2}}\\&+ \left(\beta_3|u|^2 + \beta_4|v|^2\right)u\sqrt{|u|^2 + |v|^2} + \left(\gamma_1|u|^6 + \gamma_2|u|^4|v|^2 + \gamma_3|u|^2|v|^4 + \gamma_4|v|^6\right)u = 0,\end{aligned} \tag{1}$$

$$\begin{aligned}&iv_t + ib_1v_{xxx} + b_2v_{xxxx} + \frac{b_3v}{\delta_1|v|^6 + \delta_2|v|^4|u|^2 + \delta_3|v|^2|u|^4 + \delta_4|u|^6} + \frac{b_4v}{\left(\lambda_1|v|^2 + \lambda_2|u|^2\right)\sqrt{|v|^2 + |u|^2}}\\&+ \left(\lambda_3|v|^2 + \lambda_4|u|^2\right)v\sqrt{|v|^2 + |u|^2} + \left(\mu_1|v|^6 + \mu_2|v|^4|u|^2 + \mu_3|v|^2|u|^4 + \mu_4|u|^6\right)v = 0,\end{aligned} \tag{2}$$

where $u = u(x,t)$ and $v = v(x,t)$ represent wave profiles in two components of a birefringent optical fiber. The constants a_i, b_i for $i = 1,2$ govern third-order dispersion (3OD) and fourth-order dispersion (4OD), respectively, while a_j, b_j for $j = 3,4$ and $\alpha_l, \beta_l, \gamma_l, \delta_l, \lambda_l, \mu_l$ for $l = 1,2,3,4$ describe nonlinear interactions, including self-phase modulation (SPM) and cross-phase modulation (XPM). These parameters characterize intricate wave dynamics, which are essential for comprehending soliton evolution and stability within nonlinear optical frameworks. Although the model does not retain the classical group-velocity-dispersion (second-derivative) term, it is conventionally classified within the nonlinear Schrodinger family in the optics literature: near the zero-dispersion wavelength the standard GVD coefficient vanishes, and the leading dispersive contributions become the third- and fourth-order terms retained here, giving rise to the so-called cubic-quartic nonlinear Schrodinger equation [24]. The extended trial function method has been employed in [24] to derive cubic-quartic optical soliton solutions, including bright and singular solitons, periodic solutions, and Jacobi elliptic function solutions, for specific cases of the power-law nonlinearity parameter ($n = 1,2,3$). This approach transformed the coupled system into ordinary differential equations, solved using a polynomial ansatz, and provided valuable insights into soliton dynamics under differential group delay in nonlinear optical systems. In contrast, this study builds upon the framework established by Biswas et al. by applying the modified extended mapping method (MEMM) to the same coupled system defined by Eqs. (1) and (2). Unlike the extended trial function method, which relies on a polynomial ansatz, MEMM utilizes series expansions and mapping functions to derive a broader range of exact solutions, including solitons, periodic waves, and singular structures. This approach enhances the flexibility in handling the complex nonlinearities and higher-order dispersions inherent in the system, potentially yielding novel solutions not captured by the extended trial function method. By leveraging MEMM, this research aims to provide a more comprehensive set of analytical solutions, offering deeper insights into wave stability, interaction dynamics, and their applications in optimizing optical communication systems. The study also includes graphical representations and bifurcation analysis to validate the solutions and explore qualitative transitions in wave behavior, further distinguishing it from the work of Biswas et al. The motivation for this study stems from the need to advance our understanding of complex wave interactions in nonlinear optical systems, particularly through the exploration of coupled nonlinear partial differential equations (NPDEs) like Eqs. (1) and (2). These equations model intricate phenomena in birefringent optical fibers, where cubic-quartic dispersions and higher-order nonlinearities, such as those described by Kudryashov's law, govern soliton dynamics. By applying the modified extended mapping method (MEMM), this research aims to derive novel exact wave solutions, including solitons and periodic waves, that—together with bifurcation analysis—offer deeper insights into wave stability, interaction patterns, and critical parameter-induced transitions under differential group delay. These results are critical for optimizing optical communication systems, enhancing signal transmission robustness, and addressing challenges in nonlinear optics, thereby contributing to both theoretical advancements and practical applications in high-speed data transfer and photonics.

The manuscript is structured into six principal parts. Section 1 furnishes an introduction, describing the background and aims. Section 2 elaborates on the MEMM methodology. Section 3 delineates exact solutions for the coupled model. Section 4 offers graphical illustrations to depict the results. Section 5 delivers the bifurcation analysis, and Section 6 summarizes the work and discusses its implications for nonlinear optics and allied domains.

2. MODIFIED EXTENDED MAPPING METHOD

The MEMM provides a powerful and systematic procedure for deriving exact traveling-wave solutions of NPDEs [25]. The main steps of the method are described as follows:

Phase I: Consider a general NPDE expressed as:

$$F(u, u_t, u_x, u_{xx}, u_{xxx}, u_{xxxx}, u_{xxxxx}, \dots) = 0, \tag{3}$$

where $u = u(x,t)$ is the unknown function and F is a polynomial in u and its partial derivatives.

Phase II: Introduce the wave transformation

$$u(x,t) = \Phi(\xi), \quad \xi = x - at, \quad a \in \mathbb{R} - \{0\}, \tag{4}$$

in which a denotes the wave speed. Substituting (4) into (3) reduces the equation to an ordinary differential equation (ODE)

$$G(\Phi, \Phi', \Phi'', \Phi''', \dots) = 0. \tag{5}$$

Phase III: Assume a solution of the form

$$\Phi(\xi) = \sum_{i=0}^{N} p_i\, \mathcal{W}^i(\xi) + \sum_{i=1}^{N} q_i\, \mathcal{W}^{-i}(\xi) + \sum_{i=2}^{N} r_i\, \mathcal{W}^{i-2}(\xi)\, \mathcal{W}'(\xi) + \sum_{i=1}^{N} s_i\, \frac{\mathcal{W}'(\xi)}{\mathcal{W}^i(\xi)}, \tag{6}$$

where p_i, q_i, r_i, and s_i are constants to be determined, and the auxiliary function $\mathcal{W}(\xi)$ satisfies

$$\mathcal{W}'(\xi) = \sqrt{c_0 + c_1\mathcal{W} + c_2\mathcal{W}^2 + c_3\mathcal{W}^3 + c_4\mathcal{W}^4 + c_5\mathcal{W}^6}, \tag{7}$$

with real coefficients c_j $(j = 0, 1, \dots, 5)$.
Phase IV: Determine the positive integer N by balancing the highest-order derivative term with the leading nonlinear term in the ODE (5).
Phase V: Insert the ansatz (6) together with the relation (7) into the ODE (5). This yields a polynomial in powers of $\mathcal{W}$ (and terms involving $\mathcal{W}'$). Setting the coefficients of all independent terms to zero produces a system of algebraic equations for the unknowns p_i, q_i, r_i, s_i, a and the parameters c_j. Solving this system using symbolic software such as Maple, Mathematica, or MATLAB delivers explicit parameter values, from which a broad spectrum of exact solutions—including hyperbolic, trigonometric, elliptic, exponential, and rational functions—are obtained for the original NPDE (3).

3. CONSTRUCTION OF EXACT SOLUTIONS

In this section, the Modified Extended Mapping Method (MEMM) is systematically applied to construct exact traveling wave solutions for the coupled Kudryashov's system, Eqs. (1) and (2). The derivation begins with the standard traveling wave reduction introduced in the previous section. Subsequently, the core algorithm of the MEMM is implemented to obtain a spectrum of closed-form analytical solutions. The solutions are in the form:

$$\begin{aligned} u(x,t) &= U(\xi)\, e^{i(-kx+\omega t+\theta)}, \\ v(x,t) &= V(\xi)\, e^{i(-kx+\omega t+\theta)}, \end{aligned} \tag{8}$$

and

$$\xi = x - c\,t, \tag{9}$$

with θ, k, ω, and c being non-zero constants; here c stands for the wave propagation speed, k signifies the frequency, ω indicates the wave number, and θ denotes the phase constant. We begin by applying the wave ansatz given in Eqs. (8) to Eqs. (1) and (2), and subsequently separate the real and imaginary components, which generate the equations that follow

$$\begin{aligned} \mathrm{Re}_1: \quad & a_2U^{(4)}(\xi) + \left(3ka_1 - 6k^2a_2\right) U''(\xi) + \gamma_1U^7(\xi) + \gamma_2U^5(\xi)V^2(\xi) + \gamma_3U^3(\xi)V^4(\xi) + \gamma_4U(\xi)V^6(\xi) \\ & + \beta_3U^3(\xi)\sqrt{U^2(\xi)+V^2(\xi)} + \beta_4U(\xi)V^2(\xi)\sqrt{U^2(\xi)+V^2(\xi)} + \left(-\omega - k^3a_1 + k^4a_2\right) U(\xi) + \\ & \frac{a_4U(\xi)}{\sqrt{U^2(\xi)+V^2(\xi)}\,\left(\beta_1U^2(\xi)+\beta_2V^2(\xi)\right)} + \frac{a_3U(\xi)}{\alpha_1U^6(\xi)+\alpha_2U^4(\xi)V^2(\xi)+\alpha_3U^2(\xi)V^4(\xi)+\alpha_4V^6(\xi)} = 0, \end{aligned} \tag{10}$$

$$\begin{aligned} \mathrm{Re}_2: \quad & b_2V^{(4)}(\xi) + \left(3kb_1 - 6k^2b_2\right) V''(\xi) + \mu_1V^7(\xi) + \mu_2U^2(\xi)V^5(\xi) + \mu_3U^4(\xi)V^3(\xi) + \mu_4U^6(\xi)V(\xi) \\ & + \lambda_3V^3(\xi)\sqrt{U^2(\xi)+V^2(\xi)} + \lambda_4U^2(\xi)V(\xi)\sqrt{U^2(\xi)+V^2(\xi)} + \left(-\omega - k^3b_1 + k^4b_2\right) V(\xi) + \\ & \frac{b_4V(\xi)}{\sqrt{U^2(\xi)+V^2(\xi)}\,\left(\lambda_2U^2(\xi)+\lambda_1V^2(\xi)\right)} + \frac{b_3V(\xi)}{\delta_4U^6(\xi)+\delta_3U^4(\xi)V^2(\xi)+\delta_2U^2(\xi)V^4(\xi)+\delta_1V^6(\xi)} = 0, \end{aligned} \tag{11}$$

$$\mathrm{Im}_1: \quad (-a_1 + 4ka_2)\, U^{(3)}(\xi) + \left(c + 3k^2a_1 - 4k^3a_2\right) U'(\xi) = 0, \tag{12}$$

$$\mathrm{Im}_2: \quad (-b_1 + 4kb_2)\, V^{(3)}(\xi) + \left(c + 3k^2 b_1 - 4k^3 b_2\right) V'(\xi) = 0, \tag{13}$$

Differentiating Eqs. (12) and (13) once with respect to ξ yields explicit expressions for $U^{(4)}(\xi)$ and $V^{(4)}(\xi)$, respectively; substituting these into Eqs. (10) and (11), giving

$$\begin{aligned}
\mathrm{Re}_1: \quad & \left(\frac{3ka_1^2 - 15k^2 a_1 a_2 + a_2\left(c + 20k^3 a_2\right)}{a_1 - 4ka_2}\right) U''(\xi) + \gamma_1 U^7(\xi) \; + \gamma_2 U^5(\xi) V^2(\xi) \\
& + \gamma_3 U^3(\xi) V^4(\xi) + \gamma_4 U(\xi) V^6(\xi) + \beta_3 U^3(\xi)\sqrt{U^2(\xi) + V^2(\xi)} + \beta_4 U(\xi) V^2(\xi)\sqrt{U^2(\xi) + V^2(\xi)} \\
& + \frac{a_4 U(\xi)}{\sqrt{U^2(\xi) + V^2(\xi)}\,\left(\beta_1 U^2(\xi) + \beta_2 V^2(\xi)\right)} + \frac{a_3 U(\xi)}{\alpha_1 U^6(\xi) + \alpha_2 U^4(\xi) V^2(\xi) + \alpha_3 U^2(\xi) V^4(\xi) + \alpha_4 V^6(\xi)} \\
& + \left(-\omega - k^3 a_1 + k^4 a_2\right) U(\xi) = 0,
\end{aligned} \tag{14}$$

$$\begin{aligned}
\mathrm{Re}_2: \quad & \left(\frac{3kb_1^2 - 15k^2 b_1 b_2 + b_2\left(c + 20k^3 b_2\right)}{b_1 - 4kb_2}\right) V''(\xi) + \mu_1 V^7(\xi) + \mu_2 U^2(\xi) V^5(\xi) \\
& + \mu_3 U^4(\xi) V^3(\xi) + \mu_4 U^6(\xi) V(\xi) + \lambda_3 V^3(\xi)\sqrt{U^2(\xi) + V^2(\xi)} + \lambda_4 U^2(\xi) V(\xi)\sqrt{U^2(\xi) + V^2(\xi)} \\
& + \frac{b_4 V(\xi)}{\sqrt{U^2(\xi) + V^2(\xi)}\,\left(\lambda_2 U^2(\xi) + \lambda_1 V^2(\xi)\right)} + \frac{b_3 V(\xi)}{\delta_4 U^6(\xi) + \delta_3 U^4(\xi) V^2(\xi) + \delta_2 U^2(\xi) V^4(\xi) + \delta_1 V^6(\xi)} \\
& + \left(-\omega - k^3 b_1 + k^4 b_2\right) V(\xi) = 0.
\end{aligned} \tag{15}$$

Let

$$V(\xi) = A\, U(\xi), \tag{16}$$

under the condition $A \neq \{0, 1\}$. Then, Eqs. (14) and (15) can be rewritten as

$$\begin{aligned}
& \left(\frac{3ka_1^2 - 15k^2 a_1 a_2 + a_2(c + 20k^3 a_2)}{a_1 - 4ka_2}\right) U^5(\xi) U''(\xi) + \left(\gamma_1 + A^2\gamma_2 + A^4\gamma_3 + A^6\gamma_4\right) U(\xi)^{12} \\
& + \sqrt{1 + A^2}\left(\beta_3 + A^2\beta_4\right) U(\xi)^9 + \left(-\omega - k^3 a_1 + k^4 a_2\right) U^6(\xi) + \frac{a_4 U^3(\xi)}{\sqrt{1 + A^2}\,\left(\beta_1 + A^2\beta_2\right)} \\
& + \frac{a_3}{\alpha_1 + A^2\alpha_2 + A^4\alpha_3 + A^6\alpha_4} = 0,
\end{aligned} \tag{17}$$

$$\begin{aligned}
& A\left(\frac{3kb_1^2 - 15k^2 b_1 b_2 + b_2(c + 20k^3 b_2)}{b_1 - 4kb_2}\right) U^5(\xi) U''(\xi) + A\left(A^6\mu_1 + A^4\mu_2 + A^2\mu_3 + \mu_4\right) U(\xi)^{12} \\
& + A\sqrt{1 + A^2}\left(A^2\lambda_3 + \lambda_4\right) U(\xi)^9 + A\left(-\omega - k^3 b_1 + k^4 b_2\right) U^6(\xi) + \frac{A b_4 U^3(\xi)}{\sqrt{1 + A^2}\,\left(A^2\lambda_1 + \lambda_2\right)} \\
& + \frac{A b_3}{A^6\delta_1 + A^4\delta_2 + A^2\delta_3 + \delta_4} = 0.
\end{aligned} \tag{18}$$

For recovering closed form solutions, the transformation:

$$U(\xi) = F(\xi)^{\frac{1}{3}}, \tag{19}$$

is applied to Eqs. (17) and (18). Thus they change to

$$\begin{aligned}
& \left(\frac{3ka_1^2 - 15k^2 a_1 a_2 + a_2(c + 20k^3 a_2)}{9(a_1 - 4ka_2)}\right)\left(3F(\xi)F''(\xi) - 2F'(\xi)^2\right) + \left(\gamma_1 + A^2\gamma_2 + A^4\gamma_3 + A^6\gamma_4\right) F(\xi)^4 \\
& + \sqrt{1 + A^2}\left(\beta_3 + A^2\beta_4\right) F(\xi)^3 - \left(\omega + k^3 a_1 - k^4 a_2\right) F(\xi)^2 + \frac{a_4 F(\xi)}{\sqrt{1 + A^2}\,\left(\beta_1 + A^2\beta_2\right)} \\
& + \frac{a_3}{\alpha_1 + A^2\alpha_2 + A^4\alpha_3 + A^6\alpha_4} = 0,
\end{aligned} \tag{20}$$

$$A\left(\frac{3kb_1^2-15k^2b_1b_2+b_2(c+20k^3b_2)}{9(b_1-4kb_2)}\right)\left(3F(\xi)F''(\xi)-2F'(\xi)^2\right)+A\left(A^6\mu_1+A^4\mu_2+A^2\mu_3+\mu_4\right)F(\xi)^4$$
$$+A\sqrt{1+A^2}\left(A^2\lambda_3+\lambda_4\right)F(\xi)^3-A\left(\omega+k^3b_1-k^4b_2\right)F(\xi)^2+\frac{Ab_4F(\xi)}{\sqrt{1+A^2}\left(A^2\lambda_1+\lambda_2\right)}$$
$$+\frac{Ab_3}{A^6\delta_1+A^4\delta_2+A^2\delta_3+\delta_4}=0. \tag{21}$$

The previous Eqs. (20) and (21) have the same form under the following constraint conditions:

$$\left.\begin{aligned}
&\frac{3ka_1^2-15k^2a_1a_2+a_2(c+20k^3a_2)}{9(a_1-4ka_2)}=\frac{3kb_1^2-15k^2b_1b_2+b_2(c+20k^3b_2)}{9(b_1-4kb_2)},\\
&\gamma_1+A^2\gamma_2+A^4\gamma_3+A^6\gamma_4=A^6\mu_1+A^4\mu_2+A^2\mu_3+\mu_4,\\
&\sqrt{1+A^2}\left(\beta_3+A^2\beta_4\right)=\sqrt{1+A^2}\left(A^2\lambda_3+\lambda_4\right),\\
&\omega+k^3a_1-k^4a_2=\omega+k^3b_1-k^4b_2,\\
&\frac{a_4}{\sqrt{1+A^2}\left(\beta_1+A^2\beta_2\right)}=\frac{b_4}{\sqrt{1+A^2}\left(A^2\lambda_1+\lambda_2\right)},\\
&\frac{a_3}{\alpha_1+A^2\alpha_2+A^4\alpha_3+A^6\alpha_4}=\frac{b_3}{A^6\delta_1+A^4\delta_2+A^2\delta_3+\delta_4}.
\end{aligned}\right\} \tag{22}$$

Hence, Eq. (20) can be reformulated as

$$\sigma_1\left(3F(\xi)F''(\xi)-2F'(\xi)^2\right)+\sigma_2F(\xi)^4+\sigma_3F(\xi)^3-\sigma_4F(\xi)^2+\sigma_5F(\xi)+\sigma_6=0, \tag{23}$$

where

$$\begin{aligned}
&\sigma_1=\frac{3ka_1^2-15k^2a_1a_2+a_2(c+20k^3a_2)}{9(a_1-4ka_2)},\quad \sigma_2=\gamma_1+A^2\gamma_2+A^4\gamma_3+A^6\gamma_4,\\
&\sigma_3=\sqrt{1+A^2}\left(\beta_3+A^2\beta_4\right),\quad \sigma_4=\omega+k^3a_1-k^4a_2,\\
&\sigma_5=\frac{a_4}{\sqrt{1+A^2}\left(\beta_1+A^2\beta_2\right)},\quad \sigma_6=\frac{a_3}{\alpha_1+A^2\alpha_2+A^4\alpha_3+A^6\alpha_4}.
\end{aligned} \tag{24}$$

To ascertain the solution structure, the balancing method is employed on Eq. (23), which yields $N=1$. Accordingly, following Eq. (6), the function $F(\xi)$ takes the form:

$$F(\xi)=p_0+p_1\mathcal{W}(\xi)+q_1\frac{1}{\mathcal{W}(\xi)}+s_1\frac{\mathcal{W}'(\xi)}{\mathcal{W}(\xi)}, \tag{25}$$

in which p_0, p_1, q_1, and s_1 represent undetermined constants. Substituting $F(\xi)$ from Eq. (25) together with Eq. (7) into Eq. (23), we collect the coefficients corresponding to $\mathcal{W}^i$ for $i\in[-4,8]$, $\mathcal{W}^j\mathcal{W}'$ for $j\in[-4,4]$, $\mathcal{W}^k\mathcal{W}'^2$ for $k\in[-4,0]$, $\mathcal{W}^l\mathcal{W}'^3$ for $l\in[-4,2]$, and $\mathcal{W}^{-4}\mathcal{W}'^4$. Equating all these coefficients to zero generates an algebraic system; solving this system provides the analytical solutions to Eqs. (1) and (2), presented below:

Case Study 1: $c_0=c_1=c_3=c_5=0$.
Solving the resulting algebraic system produces two consistent parameter sets.

[1.1] $p_0=-\dfrac{2\sigma_3}{5\sigma_2}$, $p_1=\dfrac{\sqrt{-8c_4\sigma_3^4-625c_4\sigma_2^3\sigma_6}}{5\sqrt{2c_2}\sigma_2\sigma_3}$, $q_1=0$, $s_1=0$, $\sigma_1=\dfrac{8\sigma_3^4+625\sigma_2^3\sigma_6}{200c_2\sigma_2\sigma_3^2}$, $\sigma_4=\dfrac{-8\sigma_3^4+125\sigma_2^3\sigma_6}{40\sigma_2\sigma_3^2}$, $\sigma_5=\dfrac{-8\sigma_3^4+625\sigma_2^3\sigma_6}{500\sigma_2^2\sigma_3}$.

[1.2] $p_0=-\dfrac{2\sigma_3}{5\sigma_2}$, $p_1=\dfrac{2\sqrt{-c_4\sigma_1}}{\sqrt{\sigma_2}}$, $q_1=0$, $s_1=0$, $\sigma_4=\dfrac{25c_2\sigma_1\sigma_2-6\sigma_3^2}{25\sigma_2}$, $\sigma_5=\dfrac{2(25c_2\sigma_1\sigma_2\sigma_3-2\sigma_3^3)}{125\sigma_2^2}$, $\sigma_6=\dfrac{8(25c_2\sigma_1\sigma_2\sigma_3^2-\sigma_3^4)}{625\sigma_2^3}$.

From subcase [1.1] the following explicit solutions are obtained:
[1.1.1] If $c_2 > 0$, $c_4 < 0$, $\sigma_2\sigma_3 \neq 0$, and $(8\sigma_3^4 + 625\sigma_2^3\sigma_6) > 0$, then

$$u_{1.1.1}(x,t) = \frac{1}{(10\sigma_2\sigma_3)^{1/3}}\left(-4\sigma_3^2 + \sqrt{2\left(8\sigma_3^4 + 625\sigma_2^3\sigma_6\right)}\,\mathrm{sech}\left[\sqrt{c_2}(x-ct)\right]\right)^{1/3} e^{-i(kx-\theta-t\omega)}, \tag{26}$$

$$v_{1.1.1}(x,t) = \frac{A}{(10\sigma_2\sigma_3)^{1/3}}\left(-4\sigma_3^2 + \sqrt{2\left(8\sigma_3^4 + 625\sigma_2^3\sigma_6\right)}\,\mathrm{sech}\left[\sqrt{c_2}(x-ct)\right]\right)^{1/3} e^{-i(kx-\theta-t\omega)}, \tag{27}$$

represent bright soliton waveforms.

[1.1.2] If $c_2 < 0$, $c_4 > 0$, $\sigma_2\sigma_3 \neq 0$, and $(8\sigma_3^4 + 625\sigma_2^3\sigma_6) > 0$, then

$$u_{1.1.2}(x,t) = \frac{1}{(10\sigma_2\sigma_3)^{1/3}}\left(-4\sigma_3^2 - \sqrt{2\left(8\sigma_3^4 + 625\sigma_2^3\sigma_6\right)}\,\sec\left[\sqrt{-c_2}(x-ct)\right]\right)^{1/3} e^{-i(kx-\theta-t\omega)}, \tag{28}$$

$$v_{1.1.2}(x,t) = \frac{A}{(10\sigma_2\sigma_3)^{1/3}}\left(-4\sigma_3^2 - \sqrt{2\left(8\sigma_3^4 + 625\sigma_2^3\sigma_6\right)}\,\sec\left[\sqrt{-c_2}(x-ct)\right]\right)^{1/3} e^{-i(kx-\theta-t\omega)}, \tag{29}$$

correspond to singular periodic waveforms.

[1.1.3] If $c_2 < 0$, $c_4 > 0$, $\sigma_2\sigma_3 \neq 0$, and $(8\sigma_3^4 + 625\sigma_2^3\sigma_6) > 0$, then

$$u_{1.1.3}(x,t) = \frac{1}{(10\sigma_2\sigma_3)^{1/3}}\left(-4\sigma_3^2 - \sqrt{2\left(8\sigma_3^4 + 625\sigma_2^3\sigma_6\right)}\,\csc\left[\sqrt{-c_2}(x-ct)\right]\right)^{1/3} e^{-i(kx-\theta-t\omega)}, \tag{30}$$

$$v_{1.1.3}(x,t) = \frac{A}{(10\sigma_2\sigma_3)^{1/3}}\left(-4\sigma_3^2 - \sqrt{2\left(8\sigma_3^4 + 625\sigma_2^3\sigma_6\right)}\,\csc\left[\sqrt{-c_2}(x-ct)\right]\right)^{1/3} e^{-i(kx-\theta-t\omega)}, \tag{31}$$

correspond to singular periodic waveforms.

From subcase [1.2] the following explicit solutions are obtained:
[1.2.1] If $c_2 > 0$, $c_4 < 0$, $\sigma_1 < 0$, and $\sigma_2 > 0$, then

$$u_{1.2.1}(x,t) = \left(\frac{2}{5\sigma_2}\right)^{1/3}\left(5\sqrt{c_2\sigma_1\sigma_2}\,\mathrm{sech}\left[\sqrt{c_2}(x-ct)\right] - \sigma_3\right)^{1/3} e^{-i(kx-\theta-t\omega)}, \tag{32}$$

$$v_{1.2.1}(x,t) = A\left(\frac{2}{5\sigma_2}\right)^{1/3}\left(5\sqrt{c_2\sigma_1\sigma_2}\,\mathrm{sech}\left[\sqrt{c_2}(x-ct)\right] - \sigma_3\right)^{1/3} e^{-i(kx-\theta-t\omega)}, \tag{33}$$

represent bright soliton waveforms.

[1.2.2] If $c_2 < 0$, $c_4 > 0$, $\sigma_1 < 0$, and $\sigma_2 > 0$, then

$$u_{1.2.2}(x,t) = \left(\frac{2}{5\sigma_2}\right)^{1/3}\left(5\sqrt{c_2\sigma_1\sigma_2}\,\sec\left[\sqrt{-c_2}(x-ct)\right] - \sigma_3\right)^{1/3} e^{-i(kx-\theta-t\omega)}, \tag{34}$$

$$v_{1.2.2}(x,t) = A\left(\frac{2}{5\sigma_2}\right)^{1/3}\left(5\sqrt{c_2\sigma_1\sigma_2}\,\sec\left[\sqrt{-c_2}(x-ct)\right] - \sigma_3\right)^{1/3} e^{-i(kx-\theta-t\omega)}, \tag{35}$$

correspond to singular periodic waveforms.

[1.2.3] If $c_2 < 0$, $c_4 > 0$, $\sigma_1 < 0$, and $\sigma_2 > 0$, then

$$u_{1.2.3}(x,t) = \left(\frac{2}{5\sigma_2}\right)^{1/3}\left(5\sqrt{c_2\sigma_1\sigma_2}\,\csc\left[\sqrt{-c_2}(x-ct)\right] - \sigma_3\right)^{1/3} e^{-i(kx-\theta-t\omega)}, \tag{36}$$

$$v_{1.2.3}(x,t) = A\left(\frac{2}{5\sigma_2}\right)^{1/3}\left(5\sqrt{c_2\sigma_1\sigma_2}\,\csc\left[\sqrt{-c_2}(x-ct)\right] - \sigma_3\right)^{1/3} e^{-i(kx-\theta-t\omega)}, \tag{37}$$

correspond to singular periodic waveforms.

Case Study 2: $c_1 = c_3 = c_5 = 0$.
Solving the resulting algebraic system produces three consistent parameter sets.

[2.1] $p_0 = -\frac{2\sigma_3}{5\sigma_2}$, $p_1 = \pm\frac{2\sqrt{-c_4\sigma_1}}{\sqrt{\sigma_2}}$, $q_1 = 0$, $s_1 = 0$, $\sigma_4 = \frac{25c_2\sigma_1\sigma_2 - 6\sigma_3^2}{25\sigma_2}$, $\sigma_5 = \frac{2(25c_2\sigma_1\sigma_2\sigma_3 - 2\sigma_3^3)}{125\sigma_2^2}$,
$\sigma_6 = -\frac{2(25c_2\sigma_1\sigma_2 - 2\sigma_3^2)^2}{625\sigma_2^3}$.

[2.2] $p_0 = -\frac{2\sigma_3}{5\sigma_2}$, $p_1 = 0$, $q_1 = \pm\frac{c_2\sqrt{-\sigma_1}}{\sqrt{c_4\sigma_2}}$, $s_1 = 0$, $\sigma_4 = -\frac{2(25c_2\sigma_1\sigma_2 + 3\sigma_3^2)}{25\sigma_2}$,
$\sigma_5 = -\frac{4(25c_2\sigma_1\sigma_2\sigma_3 + \sigma_3^3)}{125\sigma_2^2}$, $\sigma_6 = -\frac{8(50c_2\sigma_1\sigma_2\sigma_3^2 + \sigma_3^4)}{625\sigma_2^3}$.

[2.3] $p_0 = -\frac{2\sigma_3}{5\sigma_2}$, $p_1 = \pm\frac{2\sqrt{-c_4\sigma_1}}{\sqrt{\sigma_2}}$, $q_1 = \pm\frac{c_2\sqrt{-\sigma_1}}{\sqrt{c_4\sigma_2}}$, $s_1 = 0$, $\sigma_4 = -\frac{2(25c_2\sigma_1\sigma_2 + 3\sigma_3^2)}{25\sigma_2}$,
$\sigma_5 = -\frac{4(25c_2\sigma_1\sigma_2\sigma_3 + \sigma_3^3)}{125\sigma_2^2}$, $\sigma_6 = -\frac{8(50c_2\sigma_1\sigma_2\sigma_3^2 + \sigma_3^4)}{625\sigma_2^3}$.

From subcase [2.1] the following explicit solutions are obtained:

[2.1.1] If $c_2 < 0$, $c_4 > 0$, $\sigma_1 < 0$, $\sigma_2 > 0$, and $c_0 = \frac{c_2^2}{4c_4}$, then

$$u_{2.1.1}(x,t) = \frac{1}{(5\sigma_2)^{1/3}}\left(-2\sigma_3 \pm 5\sqrt{2c_2\sigma_1\sigma_2}\tanh\left[\frac{\sqrt{-c_2}(x-ct)}{\sqrt{2}}\right]\right)^{1/3} e^{-i(kx-\theta-t\omega)}, \tag{38}$$

$$v_{2.1.1}(x,t) = \frac{A}{(5\sigma_2)^{1/3}}\left(-2\sigma_3 \pm 5\sqrt{2c_2\sigma_1\sigma_2}\tanh\left[\frac{\sqrt{-c_2}(x-ct)}{\sqrt{2}}\right]\right)^{1/3} e^{-i(kx-\theta-t\omega)}, \tag{39}$$

represent dark soliton waveforms.

[2.1.2] If $c_2 > 0$, $c_4 > 0$, $\sigma_1 < 0$, $\sigma_2 > 0$, and $c_0 = \frac{c_2^2}{4c_4}$, then

$$u_{2.1.2}(x,t) = \frac{1}{(5\sigma_2)^{1/3}}\left(-2\sigma_3 \pm 5\sqrt{-2c_2\sigma_1\sigma_2}\tan\left[\frac{\sqrt{c_2}(x-ct)}{\sqrt{2}}\right]\right)^{1/3} e^{-i(kx-\theta-t\omega)}, \tag{40}$$

$$v_{2.1.2}(x,t) = \frac{A}{(5\sigma_2)^{1/3}}\left(-2\sigma_3 \pm 5\sqrt{-2c_2\sigma_1\sigma_2}\tan\left[\frac{\sqrt{c_2}(x-ct)}{\sqrt{2}}\right]\right)^{1/3} e^{-i(kx-\theta-t\omega)}, \tag{41}$$

correspond to singular periodic waveforms.

From subcase [2.2] the following explicit solutions are obtained:

[2.2.1] If $c_2 < 0$, $c_4 > 0$, $\sigma_1 < 0$, $\sigma_2 > 0$, and $c_0 = \frac{c_2^2}{4c_4}$, then

$$u_{2.2.1}(x,t) = \frac{1}{(5\sigma_2)^{1/3}}\left(-2\sigma_3 \pm 5\sqrt{2c_2\sigma_1\sigma_2}\coth\left[\frac{\sqrt{-c_2}(x-ct)}{\sqrt{2}}\right]\right)^{1/3} e^{-i(kx-\theta-t\omega)}, \tag{42}$$

$$v_{2.2.1}(x,t) = \frac{A}{(5\sigma_2)^{1/3}}\left(-2\sigma_3 \pm 5\sqrt{2c_2\sigma_1\sigma_2}\coth\left[\frac{\sqrt{-c_2}(x-ct)}{\sqrt{2}}\right]\right)^{1/3} e^{-i(kx-\theta-t\omega)}, \tag{43}$$

correspond to singular soliton waveforms.

[2.2.2] If $c_2 > 0$, $c_4 > 0$, $\sigma_1 < 0$, $\sigma_2 > 0$, and $c_0 = \frac{c_2^2}{4c_4}$, then

$$u_{2.2.2}(x,t) = \frac{1}{(5\sigma_2)^{1/3}}\left(-2\sigma_3 \pm 5\sqrt{-2c_2\sigma_1\sigma_2}\cot\left[\frac{\sqrt{c_2}(x-ct)}{\sqrt{2}}\right]\right)^{1/3} e^{-i(kx-\theta-t\omega)}, \tag{44}$$

$$v_{2.2.2}(x,t) = \frac{A}{(5\sigma_2)^{1/3}} \left(-2\sigma_3 \pm 5\sqrt{-2c_2\sigma_1\sigma_2} \cot\left[\frac{\sqrt{c_2}(x-ct)}{\sqrt{2}} \right] \right)^{1/3} e^{-i(kx-\theta-t\omega)}, \tag{45}$$

correspond to singular periodic waveforms.

From subcase [2.3] the following explicit solutions are obtained:

[2.3.1] If $c_2 < 0$, $c_4 > 0$, $\sigma_1 < 0$, $\sigma_2 > 0$, and $c_0 = \dfrac{c_2^2}{4c_4}$, then

$$u_{2.3.1}(x,t) = \frac{1}{(5\sigma_2)^{1/3}} \left(-2\sigma_3 \pm 5\sqrt{2c_2\sigma_1\sigma_2} \left(\coth\left[\frac{\sqrt{-c_2}(x-ct)}{\sqrt{2}} \right] + \tanh\left[\frac{\sqrt{-c_2}(x-ct)}{\sqrt{2}} \right] \right) \right)^{1/3} e^{-i(kx-\theta-t\omega)}, \tag{46}$$

$$v_{2.3.1}(x,t) = \frac{A}{(5\sigma_2)^{1/3}} \left(-2\sigma_3 \pm 5\sqrt{2c_2\sigma_1\sigma_2} \left(\coth\left[\frac{\sqrt{-c_2}(x-ct)}{\sqrt{2}} \right] + \tanh\left[\frac{\sqrt{-c_2}(x-ct)}{\sqrt{2}} \right] \right) \right)^{1/3} e^{-i(kx-\theta-t\omega)}, \tag{47}$$

are combo singular-dark soliton solutions.

[2.3.2] If $c_2 > 0$, $c_4 > 0$, $\sigma_1 < 0$, $\sigma_2 > 0$, and $c_0 = \dfrac{c_2^2}{4c_4}$, then

$$u_{2.3.2}(x,t) = \frac{1}{(5\sigma_2)^{1/3}} \left(-2\sigma_3 \pm 5\sqrt{-2c_2\sigma_1\sigma_2} \left(\cot\left[\frac{\sqrt{c_2}(x-ct)}{\sqrt{2}} \right] + \tan\left[\frac{\sqrt{c_2}(x-ct)}{\sqrt{2}} \right] \right) \right)^{1/3} e^{-i(kx-\theta-t\omega)}, \tag{48}$$

$$v_{2.3.2}(x,t) = \frac{A}{(5\sigma_2)^{1/3}} \left(-2\sigma_3 \pm 5\sqrt{-2c_2\sigma_1\sigma_2} \left(\cot\left[\frac{\sqrt{c_2}(x-ct)}{\sqrt{2}} \right] + \tan\left[\frac{\sqrt{c_2}(x-ct)}{\sqrt{2}} \right] \right) \right)^{1/3} e^{-i(kx-\theta-t\omega)}, \tag{49}$$

correspond to singular periodic waveforms.

Case Study 3: $c_3 = c_4 = c_5 = 0$

Solving the resulting algebraic system produces six consistent parameter sets.

[3.1] $p_0 = -\dfrac{2\sigma_5}{c_2\sigma_1 + \sigma_4}$, $p_1 = 0$, $q_1 = -\dfrac{6c_1\sigma_1\sigma_5}{c_2^2\sigma_1^2 - \sigma_4^2}$, $s_1 = 0$, $\sigma_2 = 0$, $\sigma_3 = \dfrac{5(c_2^2\sigma_1^2 - \sigma_4^2)}{12\sigma_5}$, $\sigma_6 = \dfrac{8(2c_2\sigma_1 + \sigma_4)\sigma_5^2}{3(c_2\sigma_1 + \sigma_4)^2}$.

[3.2] $p_0 = -\dfrac{5(c_2\sigma_1 - \sigma_4)}{6\sigma_3}$, $p_1 = 0$, $q_1 = -\dfrac{5c_1\sigma_1}{2\sigma_3}$, $s_1 = 0$, $\sigma_2 = 0$, $\sigma_5 = \dfrac{5(c_2^2\sigma_1^2 - \sigma_4^2)}{12\sigma_3}$,
$\sigma_6 = \dfrac{25(c_2\sigma_1 - \sigma_4)^2(2c_2\sigma_1 + \sigma_4)}{54\sigma_3^2}$.

[3.3] $p_0 = -\dfrac{2\sigma_3}{5\sigma_2}$, $p_1 = 0$, $q_1 = \dfrac{2\sqrt{-c_0\sigma_1}}{\sqrt{\sigma_2}}$, $s_1 = 0$, $\sigma_4 = \dfrac{25c_2\sigma_1\sigma_2 - 6\sigma_3^2}{25\sigma_2}$, $\sigma_5 = \dfrac{2(25c_2\sigma_1\sigma_2\sigma_3 - 2\sigma_3^3)}{125\sigma_2^2}$,
$\sigma_6 = \dfrac{8(25c_2\sigma_1\sigma_2\sigma_3^2 - \sigma_3^4)}{625\sigma_2^3}$.

[3.4] $p_0 = \dfrac{\sqrt{2(c_2\sigma_1 - \sigma_4)}}{\sqrt{3\sigma_2}}$, $p_1 = 0$, $q_1 = \dfrac{2\sqrt{-c_0\sigma_1}}{\sqrt{\sigma_2}}$, $s_1 = 0$, $\sigma_3 = -\dfrac{5\sqrt{\sigma_2(c_2\sigma_1 - \sigma_4)}}{\sqrt{6}}$,
$\sigma_5 = \dfrac{1}{9}\left(-\dfrac{2c_2\sigma_1\sqrt{6(c_2\sigma_1 - \sigma_4)}}{\sqrt{\sigma_2}} - \dfrac{\sqrt{6(c_2\sigma_1 - \sigma_4)}\sigma_4}{\sqrt{\sigma_2}} \right)$, $\sigma_6 = \dfrac{2(5c_2^2\sigma_1^2 - 4c_2\sigma_1\sigma_4 - \sigma_4^2)}{9\sigma_2}$.

[3.5] $p_0 = \dfrac{-2\sigma_3 + \sqrt{4\sigma_3^3 + 125\sigma_2^2\sigma_5}}{5\sigma_2}$, $p_1 = 0$, $q_1 = \dfrac{c_1\sqrt{4\sigma_3^3 + 125\sigma_2^2\sigma_5}}{5c_2\sigma_2\sqrt{\sigma_3}}$, $s_1 = 0$, $\sigma_1 = \dfrac{-4\sigma_3^3 - 125\sigma_2^2\sigma_5}{25c_2\sigma_2\sigma_3}$,
$\sigma_4 = \dfrac{-8\sigma_3^3 + 125\sigma_2^2\sigma_5}{50\sigma_2\sigma_3}$, $\sigma_6 = -\dfrac{25\sigma_2\sigma_5^2}{2\sigma_3^2}$.

[3.6] $p_0 = \dfrac{5\sigma_5^2 + \sqrt{5\sigma_5(5\sigma_5^3 + \sigma_3\sigma_6^2)}}{\sigma_3\sigma_6}$, $p_1 = 0$, $q_1 = \dfrac{c_1\sqrt{5\sigma_5(5\sigma_5^3 + \sigma_3\sigma_6^2)}}{c_2\sigma_3\sigma_6}$, $s_1 = 0$, $\sigma_1 = \dfrac{2(5\sigma_5^3 + \sigma_3\sigma_6^2)}{5c_2\sigma_5\sigma_6}$,
$\sigma_2 = -\dfrac{2\sigma_3^2\sigma_6}{25\sigma_5^2}$, $\sigma_4 = \dfrac{10\sigma_5^3 - \sigma_3\sigma_6^2}{5\sigma_5\sigma_6}$.

From subcase [3.1] the following explicit solutions are obtained:
[3.1.1] If $c_2 > 0$, $(c_2^2\sigma_1^2 - \sigma_4^2) \neq 0$, and $c_0 = 0$, then

$$u_{3.1.1}(x,t) = 2^{1/3}\left(-\frac{\left(c_2\sigma_1(5+\sinh\left[\sqrt{c_2}(x-ct)\right]) - \sigma_5(-1+\sinh\left[\sqrt{c_2}(x-ct)\right])\sigma_4\right)}{(c_2^2\sigma_1^2-\sigma_4^2)(-1+\sinh\left[\sqrt{c_2}(x-ct)\right])}\right)^{1/3} e^{-i(kx-\theta-t\omega)}, \tag{50}$$

$$v_{3.1.1}(x,t) = 2^{1/3}A\left(-\frac{\left(c_2\sigma_1(5+\sinh\left[\sqrt{c_2}(x-ct)\right]) - \sigma_5(-1+\sinh\left[\sqrt{c_2}(x-ct)\right])\sigma_4\right)}{(c_2^2\sigma_1^2-\sigma_4^2)(-1+\sinh\left[\sqrt{c_2}(x-ct)\right])}\right)^{1/3} e^{-i(kx-\theta-t\omega)}, \tag{51}$$

are hyperbolic solutions.
[3.1.2] If $c_2 < 0$, $(c_2^2\sigma_1^2 - \sigma_4^2) \neq 0$, and $c_0 = 0$, then

$$u_{3.1.2}(x,t) = 2^{1/3}\left(-\frac{\sigma_5}{c_2\sigma_1+\sigma_4} - \frac{6c_2\sigma_1\sigma_5}{(c_2^2\sigma_1^2-\sigma_4^2)(-1+\sin\left[\sqrt{-c_2}(x-ct)\right])}\right)^{1/3} e^{i(-kx+\theta+t\omega)}, \tag{52}$$

$$v_{3.1.2}(x,t) = 2^{1/3}A\left(-\frac{\sigma_5}{c_2\sigma_1+\sigma_4} - \frac{6c_2\sigma_1\sigma_5}{(c_2^2\sigma_1^2-\sigma_4^2)(-1+\sin\left[\sqrt{-c_2}(x-ct)\right])}\right)^{1/3} e^{i(-kx+\theta+t\omega)}, \tag{53}$$

are periodic solutions.

From subcase [3.2] the following explicit solutions are obtained:
[3.2.1] If $c_2 > 0$, $(c_2^2\sigma_1^2 - \sigma_4^2) \neq 0$, and $c_0 = 0$, then

$$u_{3.2.1}(x,t) = 2^{1/3}\left(-\frac{\sigma_5\left(c_2\sigma_1(5+\sinh\left[\sqrt{c_2}(x-ct)\right]) - (-1+\sinh\left[\sqrt{c_2}(x-ct)\right])\sigma_4\right)}{(-1+\sinh\left[\sqrt{c_2}(x-ct)\right])(c_2^2\sigma_1^2-\sigma_4^2)}\right)^{1/3} e^{-i(kx-\theta-t\omega)}, \tag{54}$$

$$v_{3.2.1}(x,t) = 2^{1/3}A\left(-\frac{\sigma_5\left(c_2\sigma_1(5+\sinh\left[\sqrt{c_2}(x-ct)\right]) - (-1+\sinh\left[\sqrt{c_2}(x-ct)\right])\sigma_4\right)}{(-1+\sinh\left[\sqrt{c_2}(x-ct)\right])(c_2^2\sigma_1^2-\sigma_4^2)}\right)^{1/3} e^{-i(kx-\theta-t\omega)}, \tag{55}$$

are hyperbolic solutions.
[3.2.2] If $c_2 < 0$, , $\sigma_3 \neq 0$, and $c_0 = 0$, then

$$u_{3.2.2}(x,t) = \left(\frac{5}{6}\right)^{1/3}\left(-\frac{c_2\sigma_1(5+\sin\left[\sqrt{-c_2}(x-ct)\right])}{\sigma_3(-1+\sin\left[\sqrt{-c_2}(x-ct)\right])} + \frac{\sigma_4}{\sigma_3}\right)^{1/3} e^{-i(kx-\theta-t\omega)}, \tag{56}$$

$$v_{3.2.2}(x,t) = A\left(\frac{5}{6}\right)^{1/3}\left(-\frac{c_2\sigma_1(5+\sin\left[\sqrt{-c_2}(x-ct)\right])}{\sigma_3(-1+\sin\left[\sqrt{-c_2}(x-ct)\right])} + \frac{\sigma_4}{\sigma_3}\right)^{1/3} e^{-i(kx-\theta-t\omega)}, \tag{57}$$

are periodic solutions.

From subcase [3.3] the following explicit solutions are obtained:
[3.3.3] If $c_2 > 0$, $c_0 > 0$, $\sigma_1 < 0$, $\sigma_2 > 0$, and $c_1 = 0$, then

$$u_{3.3.3}(x,t) = \left(-2\sqrt{-\frac{c_2\sigma_1}{\sigma_2}}\operatorname{csch}\left[\sqrt{c_2}(x-ct)\right] + \frac{2\sigma_3}{5\sigma_2}\right)^{1/3} e^{-i(kx-\theta-t\omega)}, \tag{58}$$

$$v_{3.3.3}(x,t) = A\left(-2\sqrt{-\frac{c_2\sigma_1}{\sigma_2}}\operatorname{csch}\left[\sqrt{c_2}(x-ct)\right] + \frac{2\sigma_3}{5\sigma_2}\right)^{1/3} e^{-i(kx-\theta-t\omega)}, \tag{59}$$

correspond to singular soliton waveforms.
[3.3.4] If $c_2 < 0$, $c_0 > 0$, $\sigma_1 < 0$, $\sigma_2 > 0$, and $c_1 = 0$, then

$$u_{3.3.4}(x,t) = \left(-2\sqrt{\frac{c_2\sigma_1}{\sigma_2}}\csc\left[\sqrt{-c_2}(x-ct)\right] + \frac{2\sigma_3}{5\sigma_2}\right)^{1/3} e^{-i(kx-\theta-t\omega)}, \tag{60}$$

$$v_{3.3.4}(x,t) = A\left(-2\sqrt{\frac{c_2\sigma_1}{\sigma_2}}\csc\left[\sqrt{-c_2}(x-ct)\right] + \frac{2\sigma_3}{5\sigma_2}\right)^{1/3} e^{-i(kx-\theta-t\omega)}, \tag{61}$$

correspond to singular periodic waveforms.

From subcase [3.4] the following explicit solutions are obtained:
[3.4.3] If $c_2 > 0$, $c_0 > 0$, $\sigma_1 < 0$, $\sigma_2 > 0$, $(6c_2\sigma_1 - 6\sigma_4) > 0$, and $c_1 = 0$, then

$$u_{3.4.3}(x,t) = \frac{1}{(3\sqrt{\sigma_2})^{1/3}}\left(6\sqrt{-c_2\sigma_1}\operatorname{csch}\left[\sqrt{c_2}(x-ct)\right] + \sqrt{6c_2\sigma_1 - 6\sigma_4}\right)^{1/3} e^{-i(kx-\theta-t\omega)}, \tag{62}$$

$$v_{3.4.3}(x,t) = \frac{A}{(3\sqrt{\sigma_2})^{1/3}}\left(6\sqrt{-c_2\sigma_1}\operatorname{csch}\left[\sqrt{c_2}(x-ct)\right] + \sqrt{6c_2\sigma_1 - 6\sigma_4}\right)^{1/3} e^{-i(kx-\theta-t\omega)}, \tag{63}$$

correspond to singular soliton waveforms.
[3.4.4] If $c_2 < 0$, $c_0 > 0$, $\sigma_1 < 0$, $\sigma_2 > 0$, $(6c_2\sigma_1 - 6\sigma_4) > 0$, and $c_1 = 0$, then

$$u_{3.4.4}(x,t) = \frac{1}{(3\sqrt{\sigma_2})^{1/3}}\left(-6\sqrt{c_2\sigma_1}\csc\left[\sqrt{-c_2}(x-ct)\right] + \sqrt{6c_2\sigma_1 - 6\sigma_4}\right)^{1/3} e^{-i(kx-\theta-t\omega)}, \tag{64}$$

$$v_{3.4.4}(x,t) = \frac{A}{(3\sqrt{\sigma_2})^{1/3}}\left(-6\sqrt{c_2\sigma_1}\csc\left[\sqrt{-c_2}(x-ct)\right] + \sqrt{6c_2\sigma_1 - 6\sigma_4}\right)^{1/3} e^{-i(kx-\theta-t\omega)}, \tag{65}$$

correspond to singular periodic waveforms.

From subcase [3.5] the following explicit solutions are obtained:
[3.5.5] If $c_2 > 0$, $(4\sigma_3^3 + 125\sigma_2^2\sigma_5) > 0$, and $c_0 = \dfrac{c_1^2}{4c_2}$, then

$$u_{3.5.5}(x,t) = \frac{-1}{(5\sigma_2)^{1/3}}\left(2\sigma_3 + \frac{(c_1 + 2e^{\sqrt{c_2}(x-ct)}c_2)\sqrt{4\sigma_3^3 + 125\sigma_2^2\sigma_5}}{(c_1 - 2e^{\sqrt{c_2}(x-ct)}c_2)\sqrt{\sigma_3}}\right)e^{i(-kx+\theta+t\omega)}, \tag{66}$$

$$v_{3.5.5}(x,t) = \frac{-A}{(5\sigma_2)^{1/3}}\left(2\sigma_3 + \frac{(c_1 + 2e^{\sqrt{c_2}(x-ct)}c_2)\sqrt{4\sigma_3^3 + 125\sigma_2^2\sigma_5}}{(c_1 - 2e^{\sqrt{c_2}(x-ct)}c_2)\sqrt{\sigma_3}}\right)e^{i(-kx+\theta+t\omega)}, \tag{67}$$

are an exponential solutions.

From subcase [3.6] the following explicit solutions are obtained:
[3.6.5] If $c_2 > 0$, $\sigma_5 > 0$, $(5\sigma_5^4 + \sigma_3\sigma_5\sigma_6^2) > 0$, and $c_0 = \dfrac{c_1^2}{4c_2}$, then

$$u_{3.6.5}(x,t) = \frac{1}{(\sigma_3\sigma_6)^{1/3}}\left(5\sigma_5^2 - \frac{\sqrt{5}(c_1 + 2e^{\sqrt{c_2}(x-ct)}c_2)\sqrt{5\sigma_5^4 + \sigma_3\sigma_5\sigma_6^2}}{c_1 - 2e^{\sqrt{c_2}(x-ct)}c_2}\right)^{1/3} e^{i(-kx+\theta+t\omega)}, \tag{68}$$

$$v_{3.6.5}(x,t) = \frac{A}{(\sigma_3\sigma_6)^{1/3}}\left(5\sigma_5^2 - \frac{\sqrt{5}(c_1 + 2e^{\sqrt{c_2}(x-ct)}c_2)\sqrt{5\sigma_5^4 + \sigma_3\sigma_5\sigma_6^2}}{c_1 - 2e^{\sqrt{c_2}(x-ct)}c_2}\right)^{1/3} e^{i(-kx+\theta+t\omega)}, \tag{69}$$

are an exponential solutions.

Case Study 4: $c_0 = c_1 = c_2 = c_5 = 0$.
Solving the resulting algebraic system produces the consistent parameter set.

[4.1] $p_0 = \dfrac{-5c_3\sqrt{-\sigma_1\sigma_2} - 4\sigma_3\sqrt{c_4}}{10\sigma_2\sqrt{c_4}}$, $p_1 = -\dfrac{2\sqrt{-c_4\sigma_1}}{\sqrt{\sigma_2}}$, $q_1 = 0$, $s_1 = 0$, $\sigma_4 = -\dfrac{3(25c_3^2\sigma_1\sigma_2 + 16c_4\sigma_3^2)}{200c_4\sigma_2}$,
$\sigma_5 = \dfrac{-125c_3^3\sigma_2^{3/2}(-\sigma_1)^{3/2} - 150c_3^2\sigma_1\sigma_2\sigma_3\sqrt{c_4} - 32c_4^{3/2}\sigma_3^3}{1000c_4^{3/2}\sigma_2^2}$.

From subcase [4.1] the following explicit solutions are obtained:
[4.1.1] If $c_4 \neq 0$, $\sigma_1 < 0$, and $\sigma_2 > 0$, then

$$u_{4.1.1}(x,t) = \left(\frac{c_3\sqrt{-\sigma_1}\left((x-ct)^2c_3^2 + 12c_4\right)}{2\left(-(x-ct)^2c_3^2 + 4c_4\right)\sqrt{c_4\sigma_2}} - \frac{2\sigma_3}{5\sigma_2} \right)^{1/3} e^{i(-kx+\theta+t\omega)}, \tag{70}$$

$$v_{4.1.1}(x,t) = A\left(\frac{c_3\sqrt{-\sigma_1}\left((x-ct)^2c_3^2 + 12c_4\right)}{2\left(-(x-ct)^2c_3^2 + 4c_4\right)\sqrt{c_4\sigma_2}} - \frac{2\sigma_3}{5\sigma_2} \right)^{1/3} e^{i(-kx+\theta+t\omega)}, \tag{71}$$

are rational solutions.

Case Study 5: $c_0 = c_1 = c_5 = 0$.
Solving the resulting algebraic system produces two consistent parameter sets.

[5.1] $p_0 = \dfrac{5\sigma_5^2 + \sqrt{5\sigma_5(5\sigma_5^3 + \sigma_3\sigma_6^2)}}{\sigma_3\sigma_6}$, $p_1 = \dfrac{4c_4\sqrt{5\sigma_5(5\sigma_5^3 + \sigma_3\sigma_6^2)}}{c_3\sigma_3\sigma_6}$, $q_1 = 0$, $s_1 = 0$, $\sigma_1 = \dfrac{8(5c_4\sigma_5^3 + c_4\sigma_3\sigma_6^2)}{5c_3^2\sigma_5\sigma_6}$,
$\sigma_2 = -\dfrac{2\sigma_3^2\sigma_6}{25\sigma_5^2}$, $\sigma_4 = \dfrac{10\sigma_5^3 - \sigma_3\sigma_6^2}{5\sigma_5\sigma_6}$.
[5.2] $p_0 = \dfrac{5c_3\sqrt{-\sigma_1\sigma_2} - 4\sigma_3\sqrt{c_4}}{10\sigma_2\sqrt{c_4}}$, $p_1 = \dfrac{2\sqrt{-c_4\sigma_1}}{\sqrt{\sigma_2}}$, $q_1 = 0$, $s_1 = 0$, $\sigma_4 = -\dfrac{25c_3^2\sigma_1\sigma_2 + 48c_4\sigma_3^2}{200c_4\sigma_2}$,
$\sigma_5 = -\dfrac{25c_3^2\sigma_1\sigma_2\sigma_3 + 16c_4\sigma_3^3}{500c_4\sigma_2^2}$, $\sigma_6 = -\dfrac{(25c_3^2\sigma_1\sigma_2 + 16c_4\sigma_3^2)^2}{20000c_4^2\sigma_2^3}$.
From subcase [5.1] the following explicit solutions are obtained:
[5.1.1] If $c_2 > 0$, $\sigma_5 > 0$, $(5\sigma_5^3 + \sigma_3\sigma_6^2) > 0$, and $c_2 = \dfrac{c_3^2}{4c_4}$, then

$$\begin{aligned} u_{5.1.1}(x,t) = \left(\frac{\sqrt{\sigma_5}}{c_3^2\sigma_3\sigma_6}\right)^{1/3} & \Bigg(c_3^2\left(5\sigma_5^{3/2} + \sqrt{5(5\sigma_5^3 + \sigma_3\sigma_6^2)}\right) \\ & -4c_2c_4\sqrt{5(5\sigma_5^3 + \sigma_3\sigma_6^2)}\left(1 + \tanh\left[\frac{\sqrt{c_2}(x-ct)}{2}\right]\right)\Bigg)^{1/3} e^{-i(kx-\theta-t\omega)}, \end{aligned} \tag{72}$$

$$\begin{aligned} v_{5.1.1}(x,t) = A\left(\frac{\sqrt{\sigma_5}}{c_3^2\sigma_3\sigma_6}\right)^{1/3} & \Bigg(c_3^2\left(5\sigma_5^{3/2} + \sqrt{5(5\sigma_5^3 + \sigma_3\sigma_6^2)}\right) \\ & -4c_2c_4\sqrt{5(5\sigma_5^3 + \sigma_3\sigma_6^2)}\left(1 + \tanh\left[\frac{\sqrt{c_2}(x-ct)}{2}\right]\right)\Bigg)^{1/3} e^{-i(kx-\theta-t\omega)}, \end{aligned} \tag{73}$$

represent dark soliton waveforms.

[5.1.2] If $c_2 > 0$, $\sigma_5 > 0$, $(5\sigma_5^3 + \sigma_3\sigma_6^2) > 0$, and $c_2 = \dfrac{c_3^2}{4c_4}$, then

$$\begin{aligned} u_{5.1.2}(x,t) = \left(\frac{\sqrt{\sigma_5}}{c_3^2\sigma_3\sigma_6}\right)^{1/3} & \Bigg(c_3^2\left(5\sigma_5^{3/2} + \sqrt{5(5\sigma_5^3 + \sigma_3\sigma_6^2)}\right) \\ & -4c_2c_4\sqrt{5(5\sigma_5^3 + \sigma_3\sigma_6^2)}\left(1 + \coth\left[\frac{\sqrt{c_2}(x-ct)}{2}\right]\right)\Bigg)^{1/3} e^{-i(kx-\theta-t\omega)}, \end{aligned} \tag{74}$$

$$v_{5.1.2}(x,t) = A\left(\frac{\sqrt{\sigma_5}}{c_3^2\sigma_3\sigma_6}\right)^{1/3} \Bigg(c_3^2\left(5\sigma_5^{3/2} + \sqrt{5(5\sigma_5^3 + \sigma_3\sigma_6^2)}\right)$$

$$-4c_2c_4\sqrt{5(5\sigma_5^3+\sigma_3\sigma_6^2)}\left(1+\coth\left[\frac{\sqrt{c_2}(x-ct)}{2}\right]\right)\Bigg)^{1/3} e^{-i(kx-\theta-t\omega)}, \quad (75)$$

correspond to singular soliton waveforms.

From subcase [5.2] the following explicit solutions are obtained:

[5.2.1] If $c_2>0$, $\sigma_1<0$, $\sigma_2>0$, and $c_2=\dfrac{c_3^2}{4c_4}$, then

$$u_{5.2.1}(x,t)=\frac{1}{(10c_3\sigma_2\sqrt{c_4})^{1/3}}\Bigg(5c_3^2\sqrt{-\sigma_1\sigma_2}-4c_3\sigma_3\sqrt{c_4}$$
$$-20c_2c_4\sqrt{-\sigma_1\sigma_2}\left(1+\tanh\left[\frac{\sqrt{c_2}(x-ct)}{2}\right]\right)\Bigg)^{1/3} e^{-i(kx-\theta-t\omega)}, \quad (76)$$

$$v_{5.2.1}(x,t)=\frac{A}{(10c_3\sigma_2\sqrt{c_4})^{1/3}}\Bigg(5c_3^2\sqrt{-\sigma_1\sigma_2}-4c_3\sigma_3\sqrt{c_4}$$
$$-20c_2c_4\sqrt{-\sigma_1\sigma_2}\left(1+\tanh\left[\frac{\sqrt{c_2}(x-ct)}{2}\right]\right)\Bigg)^{1/3} e^{-i(kx-\theta-t\omega)}, \quad (77)$$

represent dark soliton waveforms.

[5.2.2] If $c_2>0$, $\sigma_1<0$, $\sigma_2>0$, and $c_2=\dfrac{c_3^2}{4c_4}$, then

$$u_{5.2.2}(x,t)=\frac{1}{(10c_3\sigma_2\sqrt{c_4})^{1/3}}\Bigg(5c_3^2\sqrt{-\sigma_1\sigma_2}-4c_3\sigma_3\sqrt{c_4}$$
$$-20c_2c_4\sqrt{-\sigma_1\sigma_2}\left(1+\coth\left[\frac{\sqrt{c_2}(x-ct)}{2}\right]\right)\Bigg)^{1/3} e^{-i(kx-\theta-t\omega)}, \quad (78)$$

$$v_{5.2.2}(x,t)=\frac{A}{(10c_3\sigma_2\sqrt{c_4})^{1/3}}\Bigg(5c_3^2\sqrt{-\sigma_1\sigma_2}-4c_3\sigma_3\sqrt{c_4}$$
$$-20c_2c_4\sqrt{-\sigma_1\sigma_2}\left(1+\coth\left[\frac{\sqrt{c_2}(x-ct)}{2}\right]\right)\Bigg)^{1/3} e^{-i(kx-\theta-t\omega)}, \quad (79)$$

correspond to singular soliton waveforms.

Case Study 6: $c_2=c_4=c_5=0$
Solving the resulting algebraic system produces two consistent parameter sets.

[6.1] $p_0=\dfrac{5\sigma_4}{6\sigma_3}$, $p_1=-\dfrac{5c_3\sigma_1}{2\sigma_3}$, $q_1=0$, $s_1=0$, $\sigma_2=0$, $\sigma_6=\dfrac{25(27c_0c_3^2\sigma_1^3+9c_1c_3\sigma_1^2\sigma_4+\sigma_4^3)}{54\sigma_3^2}$,
$\sigma_5=-\dfrac{5(3c_1c_3\sigma_1^2+\sigma_4^2)}{12\sigma_3}$.

[6.2] $p_0=\dfrac{5c_1\sqrt{-\sigma_1\sigma_2}-4\sigma_3\sqrt{c_0}}{10\sigma_2\sqrt{c_0}}$, $p_1=0$, $q_1=\dfrac{2\sqrt{-c_0\sigma_1}}{\sqrt{\sigma_2}}$, $s_1=0$, $\sigma_4=-\dfrac{3(25c_1^2\sigma_1\sigma_2+16c_0\sigma_3^2)}{200c_0\sigma_2}$,
$\sigma_5=\dfrac{125c_1^3\sigma_2^{3/2}(-\sigma_1)^{3/2}+1000c_0^2c_3\sigma_2^{3/2}(-\sigma_1)^{3/2}-150c_1^2\sigma_1\sigma_2\sigma_3\sqrt{c_0}-32\sigma_3^3c_0^{3/2}}{1000c_0^{3/2}\sigma_2^2}$.

From subcase [6.1] the following explicit solutions are obtained:
[6.1.1] If $c_3>0$, $c_0\neq 0$, and $c_1\neq 0$, then

$$u_{6.1.1}(x,t)=\left(\frac{5}{6\,\sigma_3}\right)^{1/3}\left(\sigma_4-3c_3\sigma_1\wp\left[\frac{\sqrt{c_3}}{2}(x-ct);g_1,g_2\right]\right)^{1/3} e^{i(-kx+\theta+t\omega)}, \quad (80)$$

$$v_{6.1.1}(x,t) = A\left(\frac{5}{6\sigma_3}\right)^{1/3}\left(\sigma_4 - 3c_3\sigma_1\wp\left[\frac{\sqrt{c_3}}{2}(x-ct);g_1,g_2\right]\right)^{1/3} e^{i(-kx+\theta+t\omega)}, \tag{81}$$

are Weierstrass elliptic solution, where $\wp(z;g_1,g_2)$ is the Weierstrass elliptic function with $g_1 = -\frac{4c_1}{c_3}$ and $g_2 = -\frac{4c_0}{c_3}$.

From subcase [6.2] the following explicit solutions are obtained:
[6.2.1] If $c_3 > 0$, $\sigma_1 < 0$, $\sigma_2 > 0$, $c_0 \neq 0$, and $c_1 \neq 0$, then

$$u_{6.2.1}(x,t) = \frac{1}{(10\sigma_2)^{1/3}}\left(5c_1\sqrt{-\frac{\sigma_1\sigma_2}{c_0}} - 4\sigma_3 + \frac{20\sqrt{-c_0\sigma_1\sigma_2}}{\wp\left[\frac{\sqrt{c_3}}{2}(x-ct);g_1,g_2\right]}\right)^{1/3} e^{-i(kx-\theta-t\omega)}, \tag{82}$$

$$v_{6.2.1}(x,t) = \frac{A}{(10\sigma_2)^{1/3}}\left(5c_1\sqrt{-\frac{\sigma_1\sigma_2}{c_0}} - 4\sigma_3 + \frac{20\sqrt{-c_0\sigma_1\sigma_2}}{\wp\left[\frac{\sqrt{c_3}}{2}(x-ct);g_1,g_2\right]}\right)^{1/3} e^{-i(kx-\theta-t\omega)}, \tag{83}$$

are Weierstrass elliptic solution, where $\wp(z;g_1,g_2)$ is the Weierstrass elliptic function with $g_1 = -\frac{4c_1}{c_3}$ and $g_2 = -\frac{4c_0}{c_3}$.

Case Study 7: $c_1 = c_3 = 0$.
Solving the resulting algebraic system produces three consistent parameter sets.

[7.1] $p_0 = -\frac{\sqrt{2(c_2\sigma_1-\sigma_4)}}{\sqrt{3\sigma_2}}$, $p_1 = 0$, $q_1 = -\frac{2\sqrt{c_0-\sigma_1}}{\sqrt{\sigma_2}}$, $s_1 = 0$, $\sigma_3 = \frac{5\sqrt{\sigma_2(c_2\sigma_1-\sigma_4)}}{\sqrt{6}}$, $c_5 = 0$,
$\sigma_5 = \frac{1}{9}\left(\frac{2c_2\sigma_1\sqrt{6(c_2\sigma_1-\sigma_4)}}{\sqrt{\sigma_2}} + \frac{\sigma_4\sqrt{6(c_2\sigma_1-\sigma_4)}}{\sqrt{\sigma_2}}\right)$, $\sigma_6 = \frac{2(5c_2^2\sigma_1^2 - 36c_0c_4\sigma_1^2 - 4c_2\sigma_1\sigma_4 - \sigma_4^2)}{9\sigma_2}$.

[7.2] $p_0 = -\frac{5(c_2\sigma_1-\sigma_4)}{3\sigma_3}$, $p_1 = 0$, $q_1 = -\frac{5\sqrt{-2c_0\sigma_1(c_2\sigma_1-\sigma_4)}}{\sqrt{2}\sigma_3}$, $s_1 = 0$, $\sigma_2 = \frac{6\sigma_3^2}{25(c_2\sigma_1-\sigma_4)}$,
$\sigma_5 = \frac{5(2c_2^2\sigma_1^2 - c_2\sigma_1\sigma_4 - \sigma_4^2)}{9\sigma_3}$, $\sigma_6 = \frac{25(c_2\sigma_1-\sigma_4)(5c_2^2\sigma_1^2 - 36c_0c_4\sigma_1^2 - 4c_2\sigma_1\sigma_4 - \sigma_4^2)}{27\sigma_3^2}$, $c_5 = 0$.

[7.3] $p_0 = -\frac{2\sigma_3}{5\sigma_2}$, $p_1 = 0$, $q_1 = -\frac{2\sqrt{-c_0\sigma_1}}{\sqrt{\sigma_2}}$, $s_1 = 0$, $\sigma_4 = \frac{25c_2\sigma_1\sigma_2 - 6\sigma_3^2}{25\sigma_2}$, $\sigma_5 = \frac{2(25c_2\sigma_1\sigma_2\sigma_3 - 2\sigma_3^3)}{125\sigma_2^2}$,
$\sigma_6 = -\frac{8(625c_0c_4\sigma_1^2\sigma_2^2 - 25c_2\sigma_1\sigma_2\sigma_3^2 + \sigma_3^4)}{625\sigma_2^3}$, $c_5 = 0$.

From subcase [7.1] the following explicit solutions are obtained:
[7.1.1] If $c_2 > 0$, $c_0 > 0$, $c_4 > 0$, $\sigma_1 < 0$, $\sigma_2 > 0$, and $(c_2\sigma_1 - \sigma_4) > 0$, then

$$u_{7.1.1}(x,t) = \frac{1}{3^{1/3}}\left(\frac{6c_0c_4\sigma_1}{\sqrt{-c_0c_2c_4\sigma_1\sigma_2\operatorname{csch}^2[\sqrt{c_2}(x-ct)]}} - \sqrt{\frac{6(c_2\sigma_1-\sigma_4)}{\sigma_2}}\right)^{1/3} e^{i(-kx+\theta+t\omega)}, \tag{84}$$

$$v_{7.1.1}(x,t) = \frac{A}{3^{1/3}}\left(\frac{6c_0c_4\sigma_1}{\sqrt{-c_0c_2c_4\sigma_1\sigma_2\operatorname{csch}^2[\sqrt{c_2}(x-ct)]}} - \sqrt{\frac{6(c_2\sigma_1-\sigma_4)}{\sigma_2}}\right)^{1/3} e^{i(-kx+\theta+t\omega)}, \tag{85}$$

correspond to singular soliton waveforms.

[7.1.2] If $c_2 < 0$, $c_0 > 0$, $c_4 < 0$, $\sigma_1 < 0$, $\sigma_2 > 0$, and $(c_2\sigma_1 - \sigma_4) > 0$, then

$$u_{7.1.2}(x,t) = \frac{1}{(3\sigma_2)^{1/3}}\left(\frac{6\sigma_1\sqrt{-c_0c_4\sigma_2}}{\sqrt{c_2\sigma_1\csc^2[\sqrt{-c_2}(x-ct)]}} - \sqrt{6\sigma_2(c_2\sigma_1-\sigma_4)}\right)^{1/3} e^{i(-kx+\theta+t\omega)}, \tag{86}$$

$$v_{7.1.2}(x,t) = \frac{A}{(3\sigma_2)^{1/3}}\left(\frac{6\sigma_1\sqrt{-c_0c_4\sigma_2}}{\sqrt{c_2\sigma_1\csc^2[\sqrt{-c_2}(x-ct)]}} - \sqrt{6\sigma_2(c_2\sigma_1-\sigma_4)}\right)^{1/3} e^{i(-kx+\theta+t\omega)}, \tag{87}$$

correspond to singular periodic waveforms.

From subcase [7.2] the following explicit solutions are obtained:
[7.2.1] If $c_2 > 0$, $c_0 > 0$, $c_4 > 0$, $\sigma_1 < 0$, and $(c_2\sigma_1 - \sigma_4) > 0$, then

$$u_{7.2.1}(x,t) = \left(\frac{5}{3\sigma_3}\right)^{1/3}\left(-c_2\sigma_1 + \sigma_4 - \sqrt{\frac{-6c_0c_4\sigma_1(c_2\sigma_1 - \sigma_4)}{c_2\operatorname{csch}^2\left[\sqrt{c_2}(x-ct)\right]}}\right)^{1/3} e^{i(-kx+\theta+t\omega)}, \tag{88}$$

$$v_{7.2.1}(x,t) = A\left(\frac{5}{3\sigma_3}\right)^{1/3}\left(-c_2\sigma_1 + \sigma_4 - \sqrt{\frac{-6c_0c_4\sigma_1(c_2\sigma_1 - \sigma_4)}{c_2\operatorname{csch}^2\left[\sqrt{c_2}(x-ct)\right]}}\right)^{1/3} e^{i(-kx+\theta+t\omega)}, \tag{89}$$

correspond to singular soliton waveforms.

[7.2.2] If $c_2 < 0$, $c_0 > 0$, $c_4 > 0$, $\sigma_1 < 0$, and $(c_2\sigma_1 - \sigma_4) > 0$, then

$$u_{7.2.2}(x,t) = \left(\frac{5}{3\sigma_3}\right)^{1/3}\left(-c_2\sigma_1 + \sigma_4 - \sqrt{\frac{-6c_0c_4\sigma_1(c_2\sigma_1 - \sigma_4)}{c_2\sec^2\left[\sqrt{-c_2}(x-ct)\right]}}\right)^{1/3} e^{i(-kx+\theta+t\omega)}, \tag{90}$$

$$v_{7.2.2}(x,t) = A\left(\frac{5}{3\sigma_3}\right)^{1/3}\left(-c_2\sigma_1 + \sigma_4 - \sqrt{\frac{-6c_0c_4\sigma_1(c_2\sigma_1 - \sigma_4)}{c_2\sec^2\left[\sqrt{-c_2}(x-ct)\right]}}\right)^{1/3} e^{i(-kx+\theta+t\omega)}, \tag{91}$$

correspond to singular periodic waveforms.

From subcase [7.3] the following explicit solutions are obtained:
[7.3.1] If $c_2 > 0$, $c_0 > 0$, $c_4 > 0$, $\sigma_1 < 0$, and $\sigma_2 > 0$, then

$$u_{7.3.1}(x,t) = \left(\frac{2}{5\sigma_2}\right)^{1/3}\left(-\sigma_3 - \sqrt{\frac{-25c_0c_4\sigma_1\sigma_2}{c_2\operatorname{csch}^2\left[\sqrt{c_2}(x-ct)\right]}}\right)^{1/3} e^{i(-kx+\theta+t\omega)}, \tag{92}$$

$$v_{7.3.1}(x,t) = A\left(\frac{2}{5\sigma_2}\right)^{1/3}\left(-\sigma_3 - \sqrt{\frac{-25c_0c_4\sigma_1\sigma_2}{c_2\operatorname{csch}^2\left[\sqrt{c_2}(x-ct)\right]}}\right)^{1/3} e^{i(-kx+\theta+t\omega)}, \tag{93}$$

correspond to singular soliton waveforms.

[7.3.2] If $c_2 < 0$, $c_0 > 0$, $c_4 < 0$, $\sigma_1 < 0$, and $\sigma_2 > 0$, then

$$u_{7.3.2}(x,t) = \left(\frac{2}{5\sigma_2}\right)^{1/3}\left(-\sigma_3 - \sqrt{\frac{-25c_0c_4\sigma_1\sigma_2}{c_2\csc^2\left[\sqrt{-c_2}(x-ct)\right]}}\right)^{1/3} e^{i(-kx+\theta+t\omega)}, \tag{94}$$

$$v_{7.3.2}(x,t) = A\left(\frac{2}{5\sigma_2}\right)^{1/3}\left(-\sigma_3 - \sqrt{\frac{-25c_0c_4\sigma_1\sigma_2}{c_2\csc^2\left[\sqrt{-c_2}(x-ct)\right]}}\right)^{1/3} e^{i(-kx+\theta+t\omega)}, \tag{95}$$

correspond to singular periodic waveforms.

Case Study 8: $c_1 = c_3 = c_5 = 0$.
Solving the resulting algebraic system produces two consistent parameter sets.

[8.1] $p_0 = -\dfrac{2\sigma_3}{5\sigma_2}$, $p_1 = 0$, $q_1 = \dfrac{2\sqrt{c_0 - \sigma_1}}{\sqrt{\sigma_2}}$, $s_1 = 0$, $\sigma_4 = \dfrac{25c_2\sigma_1\sigma_2 - 6\sigma_3^2}{25\sigma_2}$, $\sigma_5 = \dfrac{2(25c_2\sigma_1\sigma_2\sigma_3 - 2\sigma_3^3)}{125\sigma_2^2}$,
$\sigma_6 = -\dfrac{8(625c_0c_4\sigma_1^2\sigma_2^2 - 25c_2\sigma_1\sigma_2\sigma_3^2 + \sigma_3^4)}{625\sigma_2^3}$.

[8.2] $p_0 = -\dfrac{2\sigma_3}{5\sigma_2}$, $p_1 = \dfrac{2\sqrt{-c_4\sigma_1}}{\sqrt{\sigma_2}}$, $q_1 = \dfrac{2\sqrt{-c_0\sigma_1}}{\sqrt{\sigma_2}}$, $s_1 = 0$, $\sigma_4 = \dfrac{25c_2\sigma_1\sigma_2 - 150\sigma_1\sigma_2\sqrt{c_0c_4} - 6\sigma_3^2}{25\sigma_2}$,
$\sigma_5 = \dfrac{2(25c_2\sigma_1\sigma_2\sigma_3 - 150\sigma_1\sigma_2\sigma_3\sqrt{c_0c_4} - 2\sigma_3^3)}{125\sigma_2^2}$.

From subcase [8.1] the following Jacobi elliptic solutions are obtained:
[8.1.1] If $0 \leq m \leq 1$, $c_0 = 1$, $c_2 = -(1+m^2)$, $c_4 = m^2$, $\sigma_1 < 0$, and $\sigma_2 > 0$, then

$$u_{8.1.1}(x,t) = \left(\frac{2\sqrt{-\sigma_1}}{\sqrt{\sigma_2}\,\mathrm{cd}[(x-ct)]} - \frac{2\sigma_3}{5\sigma_2}\right)^{1/3} e^{i(-kx+\theta+t\omega)}, \tag{96}$$

$$v_{8.1.1}(x,t) = A\left(\frac{2\sqrt{-\sigma_1}}{\sqrt{\sigma_2}\,\mathrm{cd}[(x-ct)]} - \frac{2\sigma_3}{5\sigma_2}\right)^{1/3} e^{i(-kx+\theta+t\omega)}, \tag{97}$$

are Jacobi elliptic solutions.
If $m = 0$, then

$$u_{8.1.1a}(x,t) = \left(\frac{2\sqrt{-\sigma_1}\,\sec[(x-ct)]}{\sqrt{\sigma_2}} - \frac{2\sigma_3}{5\sigma_2}\right)^{1/3} e^{i(-kx+\theta+t\omega)}, \tag{98}$$

$$v_{8.1.1a}(x,t) = A\left(\frac{2\sqrt{-\sigma_1}\,\sec[(x-ct)]}{\sqrt{\sigma_2}} - \frac{2\sigma_3}{5\sigma_2}\right)^{1/3} e^{i(-kx+\theta+t\omega)}, \tag{99}$$

correspond to singular periodic waveforms.
[8.1.2] If $0 \leq m \leq 1$, $c_0 = -m^2$, $c_2 = 2m^2 - 1$, $c_4 = -m^2 + 1$, and $\sigma_1, \sigma_2 < 0$, then

$$u_{8.1.2}(x,t) = \left(\frac{2}{5}\right)^{1/3}\left(-\frac{5\,m\sqrt{\sigma_1\sigma_2} + \sigma_3\,\mathrm{nc}\,[(x-ct)]}{\sigma_2\,\mathrm{nc}\,[(x-ct)]}\right)^{1/3} e^{-i(kx-\theta-t\omega)}, \tag{100}$$

$$v_{8.1.2}(x,t) = A\left(\frac{2}{5}\right)^{1/3}\left(-\frac{5\,m\sqrt{\sigma_1\sigma_2} + \sigma_3\,\mathrm{nc}\,[(x-ct)]}{\sigma_2\,\mathrm{nc}\,[(x-ct)]}\right)^{1/3} e^{-i(kx-\theta-t\omega)}, \tag{101}$$

are Jacobi elliptic solutions.
If $m = 1$, then

$$u_{8.1.2a}(x,t) = \left(\frac{2}{5}\right)^{1/3}\left(-\frac{5\,\sqrt{\sigma_1\sigma_2}\,\mathrm{sech}[(x-ct)] + \sigma_3}{\sigma_2}\right)^{1/3} e^{-i(kx-\theta-t\omega)}, \tag{102}$$

$$v_{8.1.2a}(x,t) = A\left(\frac{2}{5}\right)^{1/3}\left(-\frac{5\,\sqrt{\sigma_1\sigma_2}\,\mathrm{sech}[(x-ct)] + \sigma_3}{\sigma_2}\right)^{1/3} e^{-i(kx-\theta-t\omega)}, \tag{103}$$

represent bright soliton waveforms.
[8.1.3] If $0 \leq m \leq 1$, $c_0 = -1$, $c_2 = -m^2 + 2$, $c_4 = m^2 - 1$, and $\sigma_1, \sigma_2 < 0$, then

$$u_{8.1.3}(x,t) = \left(\frac{2}{5}\right)^{1/3}\left(-\frac{5\sqrt{\sigma_1\sigma_2} + \sigma_3\,\mathrm{nd}[(x-ct)]}{\sigma_2\,\mathrm{nd}[(x-ct)]}\right)^{1/3} e^{-i(kx-\theta-t\omega)}, \tag{104}$$

$$v_{8.1.3}(x,t) = A\left(\frac{2}{5}\right)^{1/3}\left(-\frac{5\sqrt{\sigma_1\sigma_2} + \sigma_3\,\mathrm{nd}[(x-ct)]}{\sigma_2\,\mathrm{nd}[(x-ct)]}\right)^{1/3} e^{-i(kx-\theta-t\omega)}, \tag{105}$$

are Jacobi elliptic solutions.
If $m = 1$, then

$$u_{8.1.3a}(x,t) = \left(\frac{2}{5}\right)^{1/3}\left(-\frac{5\,\sqrt{\sigma_1\sigma_2}\,\mathrm{sech}[(x-ct)] + \sigma_3}{\sigma_2}\right)^{1/3} e^{-i(kx-\theta-t\omega)}, \tag{106}$$

$$v_{8.1.3a}(x,t) = A\left(\frac{2}{5}\right)^{1/3}\left(-\frac{5\,\sqrt{\sigma_1\sigma_2}\,\mathrm{sech}[(x-ct)] + \sigma_3}{\sigma_2}\right)^{1/3} e^{-i(kx-\theta-t\omega)}, \tag{107}$$

represent bright soliton waveforms.
[8.1.4] If $0 \leq m \leq 1$, $c_0 = \dfrac{1}{4}$, $c_2 = \dfrac{m^2}{2} - 1$, $c_4 = \dfrac{m^4}{4}$, $\sigma_1 < 0$, and $\sigma_2 > 0$, then

$$u_{8.1.4}(x,t) = \left(\frac{\sqrt{-\sigma_1}(1+\mathrm{dn}[(x-ct)])}{\sqrt{\sigma_2}\,\mathrm{sn}[(x-ct)]} - \frac{2\sigma_3}{5\sigma_2}\right)^{1/3} e^{i(-kx+\theta+t\omega)}, \tag{108}$$

$$v_{8.1.4}(x,t) = A\left(\frac{\sqrt{-\sigma_1}(1+\mathrm{dn}[(x-ct)])}{\sqrt{\sigma_2}\,\mathrm{sn}[(x-ct)]} - \frac{2\sigma_3}{5\sigma_2}\right)^{1/3} e^{i(-kx+\theta+t\omega)}, \tag{109}$$

represent Jacobi elliptic function waveforms.
When $m = 0$ or $m = 1$, we obtain singular periodic or singular soliton forms, respectively.

$$u_{8.1.4a}(x,t) = \left(\frac{2\sqrt{-\sigma_1}\csc[(x-ct)]}{\sqrt{\sigma_2}} - \frac{2\sigma_3}{5\sigma_2}\right)^{1/3} e^{i(-kx+\theta+t\omega)}, \tag{110}$$

$$v_{8.1.4a}(x,t) = A\left(\frac{2\sqrt{-\sigma_1}\csc[(x-ct)]}{\sqrt{\sigma_2}} - \frac{2\sigma_3}{5\sigma_2}\right)^{1/3} e^{i(-kx+\theta+t\omega)}, \tag{111}$$

or

$$u_{8.1.4b}(x,t) = \left(\frac{(\coth[(x-ct)] + \sqrt{-\sigma_1}\operatorname{csch}[(x-ct)])}{\sqrt{\sigma_2}} - \frac{2\sigma_3}{5\sigma_2}\right)^{1/3} e^{i(-kx+\theta+t\omega)}, \tag{112}$$

$$v_{8.1.4b}(x,t) = A\left(\frac{(\coth[(x-ct)] + \sqrt{-\sigma_1}\operatorname{csch}[(x-ct)])}{\sqrt{\sigma_2}} - \frac{2\sigma_3}{5\sigma_2}\right)^{1/3} e^{i(-kx+\theta+t\omega)}. \tag{113}$$

From subcase [8.2] the following Jacobi elliptic solutions are obtained:
[8.2.1] If $0 \le m \le 1$, $c_0 = 1$, $c_2 = -(1+m^2)$, $c_4 = m^2$, $\sigma_1 < 0$, and $\sigma_2 > 0$, then

$$u_{8.2.1}(x,t) = \left(\frac{2}{5}\right)^{1/3}\left(\frac{5\sqrt{-\sigma_1\sigma_2} + 5m\sqrt{-\sigma_1\sigma_2}\operatorname{cd}^2[(x-ct)] - \sigma_3\operatorname{cd}[(x-ct)]}{\sigma_2\operatorname{cd}[(x-ct)]}\right)^{1/3} e^{-i(kx-\theta-t\omega)}, \tag{114}$$

$$v_{8.2.1}(x,t) = A\left(\frac{2}{5}\right)^{1/3}\left(\frac{5\sqrt{-\sigma_1\sigma_2} + 5m\sqrt{-\sigma_1\sigma_2}\operatorname{cd}^2[(x-ct)] - \sigma_3\operatorname{cd}[(x-ct)]}{\sigma_2\operatorname{cd}[(x-ct)]}\right)^{1/3} e^{-i(kx-\theta-t\omega)}, \tag{115}$$

are Jacobi elliptic solutions.
If $m = 0$, then

$$u_{8.2.1a}(x,t) = \left(\frac{2\sqrt{-\sigma_1}\sec[(x-ct)]}{\sqrt{\sigma_2}} - \frac{2\sigma_3}{5\sigma_2}\right)^{1/3} e^{i(-kx+\theta+t\omega)}, \tag{116}$$

$$v_{8.2.1a}(x,t) = A\left(\frac{2\sqrt{-\sigma_1}\sec[(x-ct)]}{\sqrt{\sigma_2}} - \frac{2\sigma_3}{5\sigma_2}\right)^{1/3} e^{i(-kx+\theta+t\omega)}, \tag{117}$$

correspond to singular periodic waveforms.
[8.2.2] If $0 \le m \le 1$, $c_0 = \frac{1}{4}$, $c_2 = \frac{m^2}{2} - 1$, $c_4 = \frac{m^4}{4}$, $\sigma_1 < 0$, and $\sigma_2 > 0$, then

$$u_{8.2.2}(x,t) = \left(\frac{\sqrt{-\sigma_1}(1+\operatorname{dn}[(x-ct)])}{\sqrt{\sigma_2}\operatorname{sn}[(x-ct)]} + \frac{m^2\sqrt{-\sigma_1}\operatorname{sn}[(x-ct)]}{1+\sqrt{\sigma_2}\operatorname{dn}[(x-ct)]} - \frac{2\sigma_3}{5\sigma_2}\right)^{1/3} e^{i(-kx+\theta+t\omega)}, \tag{118}$$

$$v_{8.2.2}(x,t) = A\left(\frac{\sqrt{-\sigma_1}(1+\operatorname{dn}[(x-ct)])}{\sqrt{\sigma_2}\operatorname{sn}[(x-ct)]} + \frac{m^2\sqrt{-\sigma_1}\operatorname{sn}[(x-ct)]}{1+\sqrt{\sigma_2}\operatorname{dn}[(x-ct)]} - \frac{2\sigma_3}{5\sigma_2}\right)^{1/3} e^{i(-kx+\theta+t\omega)}, \tag{119}$$

represent Jacobi elliptic function waveforms.
When $m = 0$ or $m = 1$, we obtain singular periodic or singular soliton forms, respectively.

$$u_{8.2.2a}(x,t) = \left(\frac{2\sqrt{-\sigma_1}\csc[(x-ct)]}{\sqrt{\sigma_2}} - \frac{2\sigma_3}{5\sigma_2}\right)^{1/3} e^{i(-kx+\theta+t\omega)}, \tag{120}$$

$$v_{8.2.2a}(x,t) = A\left(\frac{2\sqrt{-\sigma_1}\csc[(x-ct)]}{\sqrt{\sigma_2}} - \frac{2\sigma_3}{5\sigma_2}\right)^{1/3} e^{i(-kx+\theta+t\omega)}, \tag{121}$$

or

$$u_{8.2.2b}(x,t) = \left(\frac{2}{5\sigma_2}\right)^{1/3}\left(5\sqrt{-\sigma_1\sigma_2}\coth[(x-ct)] - \sigma_3\right)^{1/3} e^{-i(kx-\theta-t\omega)}, \tag{122}$$

$$v_{8.2.2b}(x,t) = A\left(\frac{2}{5\sigma_2}\right)^{1/3}\left(5\sqrt{-\sigma_1\sigma_2}\coth[(x-ct)] - \sigma_3\right)^{1/3} e^{-i(kx-\theta-t\omega)}. \tag{123}$$

4. GRAPHICAL OVERVIEW

This section provides graphical illustrations of chosen exact solutions obtained in Section 3, concentrating on the amplitude distributions $|u(x,t)|$ and $|v(x,t)|$ to emphasize principal wave forms, following conventional practices in nonlinear optics to depict soliton and periodic dynamics. The visualizations include three-dimensional (3D) plots depicting spatiotemporal evolution and two-dimensional (2D) overlays illustrating wave profiles at fixed time, facilitating analysis of propagation dynamics, nonlinear interactions, and dispersion effects in the coupled (1+1)-dimensional Kudryashov's equation. The selected cases encompass a variety of solution types: bright solitons, singular periodic waves, dark solitons, singular solitons, and exponential solutions. Each figure corresponds to a specific solution type, with parameter values detailed in Table 1. These visualizations exhibit the model's capability to represent varied wave behaviors within birefringent optical waveguides, highlighting stability, periodicity, together with localization under different conditions.

Table 1. Numerical parameters employed for the depicted solutions.

Figure	Solution Form	Equations	Parameter Set
1	Bright Soliton	(26), (27)	$c = 0.65$, $k = 0.58$, $\omega = 0.05$, $\theta = 0.54$, $A = 1.95$, $\alpha_1 = 0.50$, $\alpha_2 = 0.55$, $\alpha_3 = 0.70$, $\alpha_4 = 0.90$, $\beta_3 = 0.001$, $\beta_4 = 0.05$, $\gamma_1 = 0.75$, $\gamma_2 = 0.49$, $\gamma_3 = 0.35$, $\gamma_4 = -0.25$, $c_2 = 1.15$, and $c_4 = -0.20$
2	Singular Periodic	(34), (35)	$c = 0.05$, $k = 1.95$, $\omega = 0.75$, $\theta = 0.58$, $A = 1.80$, $a_1 = -1.35$, $a_2 = 1.20$, $\beta_3 = 1.57$, $\beta_4 = 0.75$, $\gamma_1 = 1.15$, $\gamma_2 = 0.45$, $\gamma_3 = 0.75$, $\gamma_4 = 0.80$, $c_2 = -0.22$, and $c_4 = 0.2$
3	Dark Soliton	(38), (39)	$c = 0.60$, $k = 0.64$, $\omega = 0.10$, $\theta = 0.50$, $A = 1.50$, $a_1 = 0.30$, $a_2 = 0.65$, $\beta_3 = 0.03$, $\beta_4 = 0.85$, $\gamma_1 = 1.75$, $\gamma_2 = 1.45$, $\gamma_3 = 1.85$, $\gamma_4 = 2.15$, $c_2 = -0.15$, and $c_4 = 0.2$
4	Singular Soliton	(58), (59)	$c = 0.55$, $k = 0.52$, $\omega = 0.12$, $\theta = 0.65$, $A = 2.35$, $a_1 = 0.15$, $a_2 = 0.85$, $\beta_3 = 0.01$, $\beta_4 = 0.05$, $\gamma_1 = 0.25$, $\gamma_2 = 0.91$, $\gamma_3 = 0.65$, $\gamma_4 = -0.04$, $c_0 = 0.2$, and $c_2 = 0.1$.
5	Exponential	(68), (69)	$c = 0.62$, $k = 0.47$, $\omega = 0.15$, $\theta = 0.45$, $A = 1.95$, $a_3 = 1.55$, $a_4 = 1.64$, $\alpha_1 = 0.10$, $\alpha_2 = 0.48$, $\alpha_3 = 0.20$, $\alpha_4 = 0.001$, $\beta_1 = 0.65$, $\beta_2 = 4.85$, $\beta_3 = 0.15$, $\beta_4 = 0.05$, $c_1 = 0.85$, and $c_2 = 0.40$

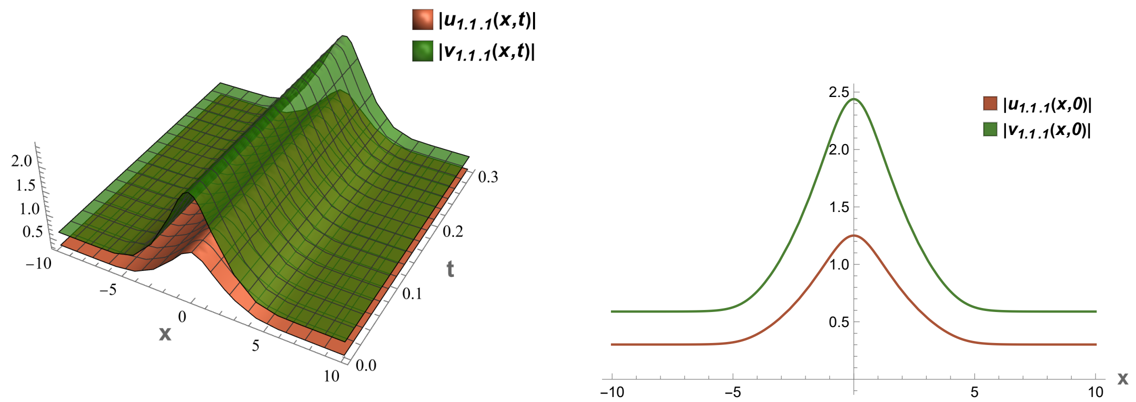

(a) 3-Dimension **(b)** 2-Dimension

Figure 1. Spatiotemporal behavior of the bright soliton wave in Eqs. (26) and (27).

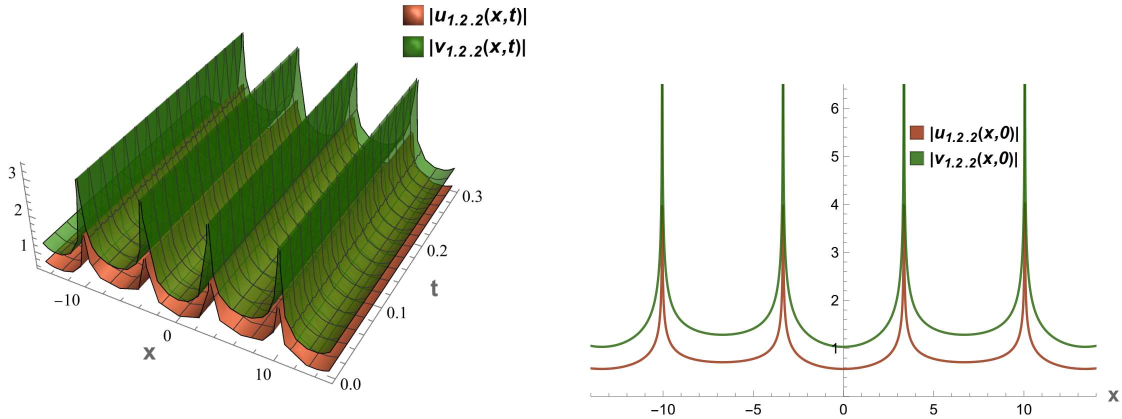

(a) 3-Dimension **(b)** 2-Dimension

Figure 2. Spatiotemporal behavior of the singular periodic wave in Eqs. (34) and (35).

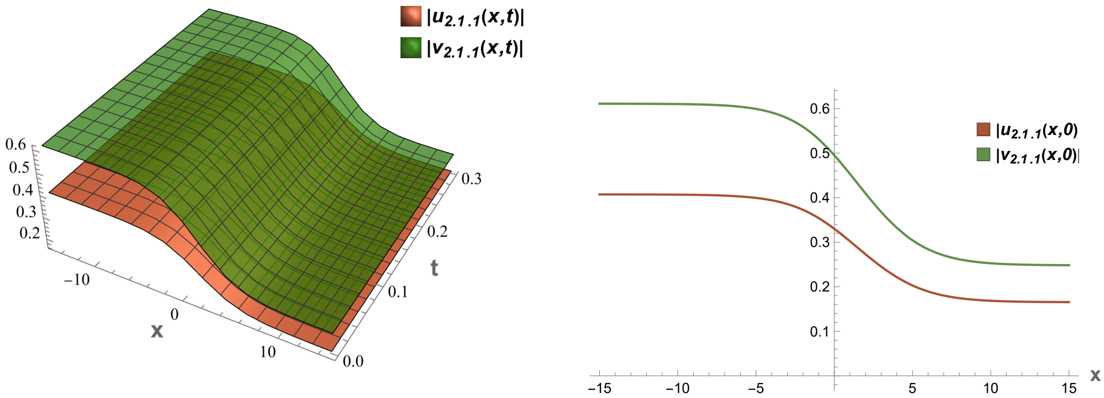

(a) 3-Dimension **(b)** 2-Dimension

Figure 3. Spatiotemporal behavior of the dark soliton wave in Eqs. (38) and (39).

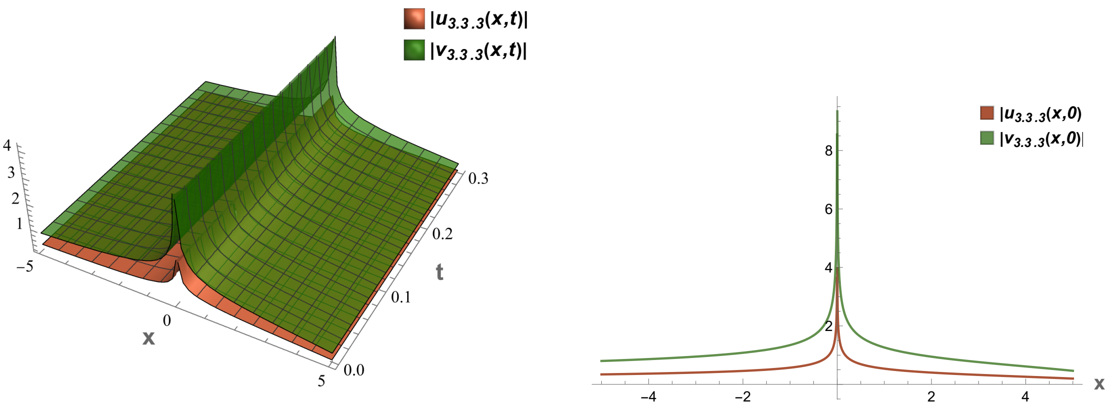

(a) 3-Dimension **(b)** 2-Dimension

Figure 4. Spatiotemporal behavior of the singular soliton wave in Eqs. (58) and (59).

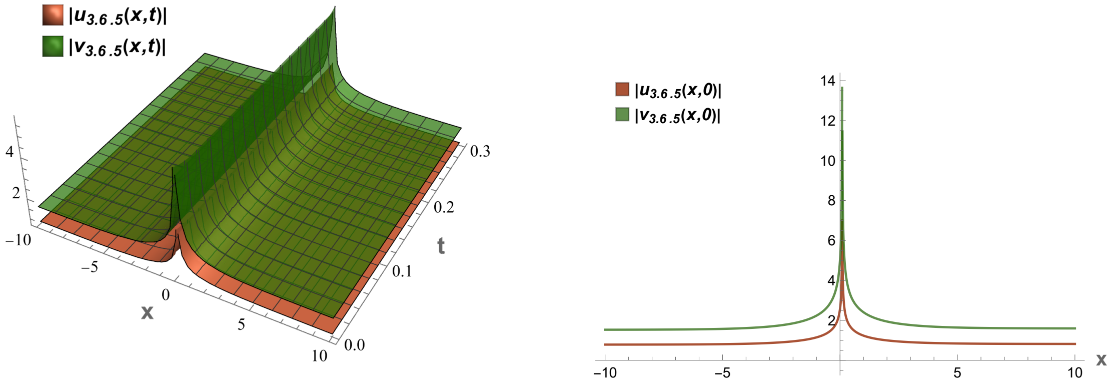

(a) 3-Dimension **(b)** 2-Dimension

Figure 5. Spatiotemporal behavior of the exponential wave in Eqs. (68) and (69).

5. BIFURCATION ANALYSIS

Bifurcation analysis provides a systematic framework for investigating qualitative changes in the dynamical behavior of nonlinear systems as parameters vary. For traveling wave equations, this approach reveals critical thresholds where solution profiles undergo transitions—for instance, between periodic and solitary waves, or between bounded and unbounded behavior [26, 27, 28, 29, 30]. In this section, we perform a detailed bifurcation analysis of the fourth-order nonlinear ordinary differential equation (23) obtained via the MEMM reduction.

5.1. Planar Dynamical System Formulation

To analyze the traveling wave dynamics, we introduce the variable $y = F'(\xi)$ and convert the second-order ODE (23) into a two-dimensional autonomous system:

$$\frac{dF}{d\xi} = y, \qquad \frac{dy}{d\xi} = \frac{2}{3}\frac{y^2}{F} - \frac{1}{3\sigma_1 F}P(F), \tag{124}$$

where $P(F) = \sigma_2 F^4 + \sigma_3 F^3 - \sigma_4 F^2 + \sigma_5 F + \sigma_6$. This system is singular along the line $F = 0$ due to the division by F. To remove this mathematical singularity while preserving the topological structure of the phase portrait, we apply the geometric singular perturbation method via the time-rescaling transformation $d\xi = F\,d\tau$. This yields the *regular* system:

$$\frac{dF}{d\tau} = Fy, \qquad \frac{dy}{d\tau} = \frac{2}{3}y^2 - \frac{1}{3\sigma_1}P(F). \tag{125}$$

Systems (124) and (125) are topologically equivalent except on the singular line $F = 0$.

5.2. Hamiltonian Structure and First Integral

System (125) is conservative and admits a Hamiltonian formulation. A first integral can be obtained via direct integration, yielding the conserved quantity

$$H(F, y) = F^{-4/3}y^2 + \frac{1}{\sigma_1}\left(\frac{\sigma_2}{4}F^{8/3} + \frac{2\sigma_3}{5}F^{5/3} - \sigma_4 F^{2/3} - 2\sigma_5 F^{-1/3} - \frac{\sigma_6}{2}F^{-4/3}\right) = h, \tag{126}$$

where h is a constant. Level curves $H(F, y) = h$ define the trajectories in the phase plane: closed orbits correspond to periodic traveling waves, homoclinic orbits to solitary waves, and heteroclinic orbits to kink or anti-kink waves.

5.3. Equilibrium Points and Linear Stability

Equilibrium points of the regular system (125) satisfy $Fy = 0$ and $\frac{2}{3}y^2 - \frac{1}{3\sigma_1}P(F) = 0$. Excluding the singular line $F = 0$, we obtain $y = 0$ and consequently $P(F) = 0$. Hence, equilibria are of the form $(F_i, 0)$, where F_i are the real roots of the quartic polynomial

$$P(F) = \sigma_2 F^4 + \sigma_3 F^3 - \sigma_4 F^2 + \sigma_5 F + \sigma_6 = 0. \tag{127}$$

The number of real equilibria can be 0, 2, or 4 (counting multiplicities), depending on the parameter values. Linearizing (125) about an equilibrium $(F_i, 0)$ gives the Jacobian matrix

$$J(F_i, 0) = \begin{bmatrix} 0 & F_i \\ -\dfrac{1}{3\sigma_1} P'(F_i) & 0 \end{bmatrix}, \tag{128}$$

where $P'(F) = 4\sigma_2 F^3 + 3\sigma_3 F^2 - 2\sigma_4 F + \sigma_5$. The characteristic equation is $\lambda^2 + \dfrac{F_i P'(F_i)}{3\sigma_1} = 0$, yielding eigenvalues

$$\lambda = \pm\sqrt{-\frac{F_i P'(F_i)}{3\sigma_1}}. \tag{129}$$

Defining $\Delta_i = -\dfrac{F_i P'(F_i)}{3\sigma_1}$, the stability type is determined as follows. When $\Delta_i > 0$, the eigenvalues are real with opposite signs, corresponding to a saddle point (unstable). When $\Delta_i < 0$, the eigenvalues are purely imaginary, corresponding to a center (stable, surrounded by periodic orbits). The degenerate case $\Delta_i = 0$ requires higher-order analysis. Because the system is conservative (Hamiltonian), centers are nonlinearly stable and give rise to families of periodic orbits.

5.4. Phase Portraits and Numerical Illustrations

To illustrate the rich dynamical behavior, we examine three representative parameter sets. For each, we compute the equilibrium points, classify their stability, and plot the phase portrait along with a sample temporal evolution.

Case 1. Parameters: $\sigma_1 = 1,\ \sigma_2 = 1,\ \sigma_3 = 0,\ \sigma_4 = 40,\ \sigma_5 = 0,\ \sigma_6 = 144$. The quartic factors as $P(F) = (F-2)(F+2)(F-6)(F+6)$, giving four equilibria: $(\pm 2, 0)$ and $(\pm 6, 0)$. Linear stability analysis shows that at $F = \pm 6$ we have $\Delta < 0$, indicating centers, while at $F = \pm 2$ we have $\Delta > 0$, indicating saddles. The phase portrait (Fig. 6a) displays two families of periodic orbits encircling the centers, separated by heteroclinic orbits connecting the saddles. The corresponding temporal profiles (Fig. 6b) exhibit periodic oscillations around $F = \pm 6$.

Case 2. Parameters: $\sigma_1 = 1,\ \sigma_2 = 1,\ \sigma_3 = 0,\ \sigma_4 = 18.25,\ \sigma_5 = 0,\ \sigma_6 = 36$. Here $P(F) = (F-4)(F+4)(F-1.5)(F+1.5)$, yielding equilibria at $(\pm 1.5, 0)$ and $(\pm 4, 0)$. Stability analysis confirms centers at $F = \pm 4$ and saddles at $F = \pm 1.5$. The phase portrait (Fig. 7a) again shows two centers surrounded by periodic orbits, with separatrices emanating from the saddles. Temporal evolution (Fig. 7b) confirms the periodic motion around the centers.

Case 3. Parameters: $\sigma_1 = 1,\ \sigma_2 = 1,\ \sigma_3 = -2,\ \sigma_4 = 45,\ \sigma_5 = -34,\ \sigma_6 = 80$. The polynomial factors as $P(F) = (F+5)(F+2)(F-1)(F-8)$, with equilibria at $(-5, 0), (-2, 0), (1, 0), (8, 0)$. Stability analysis reveals centers at $F = -5$ and $F = 8$, and saddles at $F = -2$ and $F = 1$. Despite the lack of symmetry, the phase portrait (Fig. 8a) retains the characteristic structure of two centers separated by saddle points. The temporal dynamics (Fig. 8b) display periodic oscillations around each center.

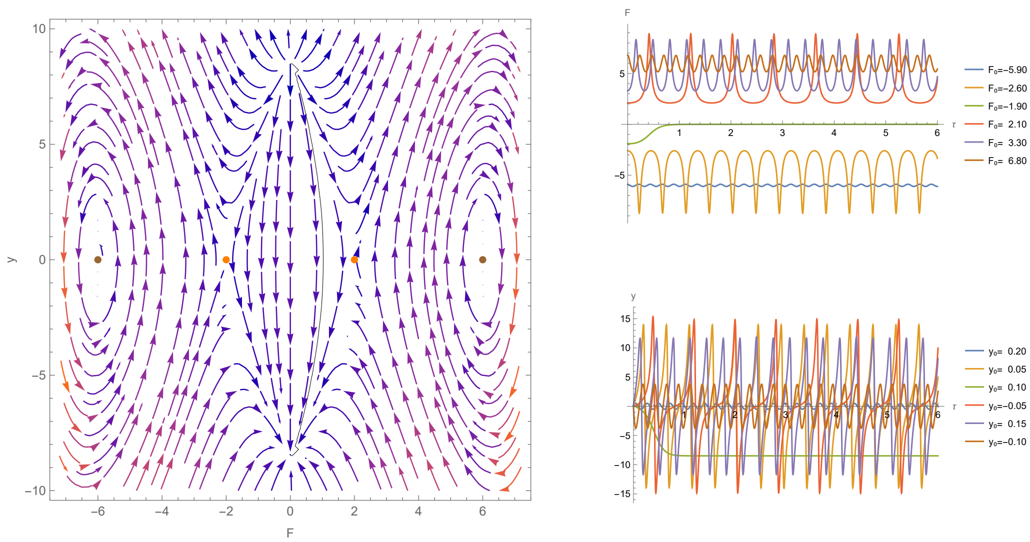

(a) Phase portrait in the (F, y)-plane for the regularized system (125).

(b) Temporal evolution of $F(\tau)$ and $y(\tau)$ for a trajectory near the center at $F = 6$.

Figure 6. Bifurcation structure for Case 1: two centers at $F = \pm 6$ and two saddles at $F = \pm 2$. Closed orbits correspond to periodic traveling waves, while the separatrices demarcate regions of distinct dynamical behavior.

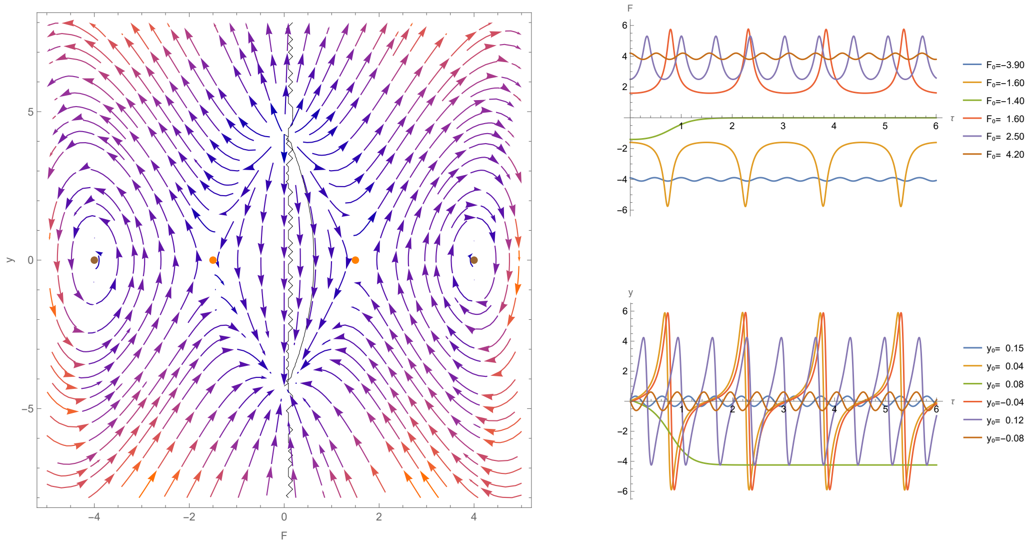

(a) Phase portrait for the regularized system (125).

(b) Temporal evolution of $F(\tau)$ and $y(\tau)$ for a periodic orbit around $F = 4$.

Figure 7. Bifurcation structure for Case 2: centers at $F = \pm 4$ and saddles at $F = \pm 1.5$. The Hamiltonian level curves generate families of periodic solutions and heteroclinic connections.

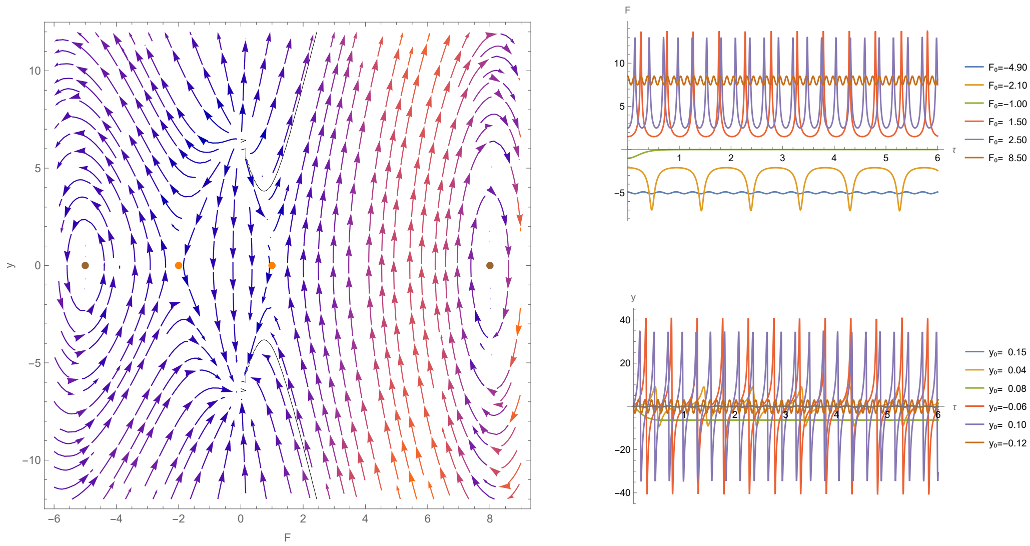

(a) Phase portrait for the regularized system (125).

(b) Temporal evolution of $F(\tau)$ and $y(\tau)$ for a trajectory near the center at $F = 8$.

Figure 8. Bifurcation structure for Case 3: centers at $F = -5$ and $F = 8$, saddles at $F = -2$ and $F = 1$. The asymmetric arrangement still yields two disjoint families of periodic orbits, illustrating the robustness of the Hamiltonian structure.

5.5. Bifurcation Interpretation

The parameter σ_6 (or any of the σ_i) can be treated as a bifurcation parameter. As it varies, the roots of $P(F)$ coalesce or split, leading to saddle-node bifurcations where equilibria appear or disappear. In a conservative system like (125), Hopf bifurcations are absent because eigenvalues are always symmetric about the imaginary axis. However, degenerate bifurcations (e.g., when $\Delta_i = 0$) may occur, leading to cusps or higher-order singularities. The phase portraits presented correspond to generic cases where all equilibria are hyperbolic (non-degenerate). The existence of periodic orbits around each center follows directly from the Hamiltonian nature and the non-degeneracy condition $\Delta_i < 0$. Moreover, the separatrices emanating from the saddles form homoclinic or heteroclinic loops, which in the original wave variable correspond to solitary wave or front solutions. In summary, the bifurcation analysis reveals that the traveling wave dynamics of the Kudryashov model are organized by a Hamiltonian planar system with up to four equilibria. The qualitative behavior—whether the wave profile is periodic, solitary, or unbounded—is determined by the level set of the Hamiltonian and the arrangement of saddles and centers. This geometric perspective complements the explicit solutions obtained via MEMM and provides a global view of the solution space.

6. CONCLUSIONS

In this research, we have successfully employed the Modified Extended Mapping Method (MEMM) to construct a comprehensive set of exact traveling wave solutions for the coupled (1+1)-dimensional Kudryashov's equation, a nonlinear partial differential equation pivotal for modeling complex wave phenomena in birefringent optical fibers. The MEMM proved to be a powerful and systematic tool, transforming the coupled nonlinear PDEs into an ordinary differential equation, thereby enabling the derivation of diverse analytical solutions. These solutions encompass a wide range of forms, including bright and singular solitons, periodic waves, rational, exponential, Weierstrass elliptic, and Jacobi elliptic functions, each capturing distinct wave dynamics relevant to applications in nonlinear optics, optical communication systems, and other nonlinear systems. The modulation instability analysis provided critical insights into the stability of steady-state solutions, highlighting the interplay between dispersion and nonlinearity. The incorporation of 3D and 2D visualizations further elucidated the spatiotemporal evolution of these solutions, offering a clear interpretation of wave propagation and interaction behaviors. This study significantly enhances the analytical framework for investigating higher-order nonlinear wave equations, providing robust tools for theoretical and applied research in nonlinear science. The analytical solutions to the coupled Kudryashov's equation offer a deeper understanding of the intricate nonlinear dynamics governed by this model, particularly in describing solitary wave interactions, periodic wave patterns, and singular structures in birefringent fibers. The diversity of solution types—ranging from hyperbolic and trigonometric to elliptic and rational forms—underscores the equation's versatility in capturing a broad spectrum of physical behaviors under various parametric conditions. The graphical representations, including 3D plots depicting wave evolution and 2D plots illustrating temporal profiles, bridge the gap between mathematical solutions and their physical implications. These visualizations highlight the MEMM's efficacy in uncovering complex wave patterns, such as soliton stability and periodic oscillations, which are critical for applications in nonlinear optics, optical communication systems, and birefringent fiber modeling. Compared to Biswas et al.'s initial study [24], which utilized the extended trial function method, the MEMM expands the solution landscape by providing new analytical solutions, including elliptic and rational solutions, thereby enhancing the theoretical comprehension of the model's integrability and dynamical behavior. However, the dependence on specific parameter constraints (e.g., c_i values) to obtain these solutions suggests potential limitations in their generalizability, particularly for arbitrary initial or boundary conditions. Additionally, the presence of singular solutions indicates regions of instability that require further investigation to assess their physical relevance. These considerations highlight the need for complementary numerical or experimental studies to validate the practical applicability of the derived solutions. This study opens several promising directions for future research. First, numerical simulations could be conducted to verify the stability and long-term behavior of the derived analytical solutions, especially under realistic physical conditions relevant to systems modeled by the Kudryashov's equation, such as birefringent fibers or optical wave propagation. Such simulations could also explore the impact of external perturbations or variable coefficients on wave dynamics. Second, extending the MEMM to other higher-order or multidimensional nonlinear PDEs, such as those in plasma physics or geophysical fluid dynamics, could further demonstrate its robustness and versatility, potentially uncovering new solution classes. Third, a deeper investigation into the integrability properties of the Kudryashov's equation using alternative techniques, such as the inverse scattering transform or Painlevé analysis, could provide additional insights into its soliton interactions and non-integrable regimes. Additionally, integrating machine learning-based approaches to approximate solutions or predict wave behaviors could complement the analytical framework, particularly for complex parameter spaces. Finally, linking the derived solutions to experimental data from relevant physical systems, such as optical fiber experiments or photonic studies, could enhance their practical utility, enabling applications in wave prediction, signal transmission optimization, or advanced material design. These prospective efforts are expected to consolidate the link bridging theoretical progress with practical implementations within nonlinear wave studies.

ORCID

Wafy M. Hasan, https://orcid.org/0000-0002-7942-6033; **Hamdy M. Ahmed**, https://orcid.org/0000-0001-8772-3663; **Ahmed M. Ahmed**, https://orcid.org/0000-0002-5829-5038; **Haytham M. Rezk**, https://orcid.org/0000-0001-6782-7908; **Wafaa B. Rabie**, https://orcid.org/0009-0001-1696-1266

REFERENCES

[1] M. D. Graham, and D. Floryan, "Exact coherent states and the nonlinear dynamics of wall-bounded turbulent flows," Annual Review of Fluid Mechanics, **53**(1), 227-253 (2021). https://doi.org/10.1146/annurev-fluid-051820-020223

[2] E. Åkervik, and M. Vartdal, "The role of wave kinematics in turbulent flow over waves," Journal of Fluid Mechanics, **880**, 890-915 (2019). https://doi.org/10.1017/jfm.2019.70810.1017/jfm.2019.708

[3] M. M. Khater, "Advanced computational techniques for solving the modified KdV-KP equation and modeling nonlinear waves," Optical and Quantum Electronics, **56**(1), 6 (2024). https://doi.org/10.1007/s11082-023-05581-3

[4] B. Kopçasız, "Qualitative analysis and optical soliton solutions galore: scrutinizing the (2+ 1)-dimensional complex modified Korteweg–de Vries system," Nonlinear Dynamics, **112**(23), 21321-21341 (2024). https://doi.org/10.1007/s11071-024-10036-9

[5] D. Moreira, P. Xavier, A. Palmeira, and E. Nascimento, "New approach to solving the atmospheric pollutant dispersion equation using fractional derivatives," International Journal of Heat and Mass Transfer, **144**, 118667 (2019). https://doi.org/10.1016/j.ijheatmasstransfer.2019.118667

[6] N. M. Jamil, and I. Khan, "Unravelling the Influence of Advection and Diffusion on the Spatial and Temporal Evolution of Pollutant Concentration," Journal of Advanced Research in Fluid Mechanics and Thermal Sciences, **119**(2), 1-12 (2024). https://doi.org/10.37934/arfmts.119.2.112

[7] U. Younas, T. A. Sulaiman, and J. Ren, "On the study of optical soliton solutions to the three-component coupled nonlinear Schrödinger equation: applications in fiber optics," Optical and Quantum Electronics, **55**(1), 72 (2023). https://doi.org/10.1007/s11082-022-04254-x

[8] M. Arshad, F. Yasin, S. F. Aldosary, H. Rezazadeh, M. Farman, and M. A. Hosseinzadeh, "Rational function solutions of higher-order dispersive cubic-quintic nonlinear Schrödinger dynamical model and its applications in fiber optics," Mathematical Methods in the Applied Sciences, **48**(4), 5300-5314 (2025). https://doi.org/10.1002/mma.10604

[9] G. A. Meehl, F. Zwiers, J. Evans, T. Knutson, L. Mearns, and P. Whetton, "Trends in extreme weather and climate events: issues related to modeling extremes in projections of future climate change," Bulletin of the American Meteorological Society, **81**(3), 427-436 (2000). https://doi.org/10.1175/1520-0477(2000)081⟨0427:TIEWAC⟩2.3.CO;2

[10] A. Moazami, V. M. Nik, S. Carlucci, and S. Geving, "Impacts of future weather data typology on building energy performance – Investigating long-term patterns of climate change and extreme weather conditions," Applied Energy, **238**, 696-720 (2019). https://doi.org/10.1016/j.apenergy.2019.01.085

[11] A. Irshad, N. Ahmed, U. Khan, S. T. Mohyud-Din, I. Khan, and E. S. M. Sherif, "Optical solutions of Schrödinger equation using extended Sinh–Gordon equation expansion method," Frontiers in Physics, **8**, 73 (2020). https://doi.org/10.3389/fphy.2020.00073

[12] H. H. Hussein, H. M. Ahmed, and W. Alexan, "Analytical soliton solutions for cubic-quartic perturbations of the Lakshmanan-Porsezian-Daniel equation using the modified extended tanh function method," Ain Shams Engineering Journal, **15**(3), 102513 (2024). https://doi.org/10.1016/j.asej.2023.102513

[13] I. A. Ibrahim, W. M. Taha, M. Alobaidi, A. F. Jameel, E. Bashier, and N. H. Alshirawi, "Oblique Closed Form Solution for Some Type Fractional Evolution Equations in Physical Problem by Using the Homogeneous Balance Method," Mathematical Modelling of Engineering Problems, **11**(1), (2024). https://doi.org/10.18280/mmep.110120

[14] A. R. Seadawy, H. M. Ahmed, W. B. Rabie, and A. Biswas, "An alternate pathway to solitons in magneto-optic waveguides with triple-power law nonlinearity," Optik, **231**, 166480 (2021). https://doi.org/10.1016/j.ijleo.2021.166480

[15] Y. Alhojilan, H. M. Ahmed, and W. B. Rabie, "Stochastic solitons in birefringent fibers for Biswas–Arshed equation with multiplicative white noise via Itô calculus by modified extended mapping method," Symmetry, **15**(1), 207 (2023). https://doi.org/10.3390/sym15010207

[16] W. B. Rabie, H. M. Ahmed, I. Samir, and M. Alnahhass, "Optical solitons and stability analysis for NLSE with nonlocal nonlinearity, nonlinear chromatic dispersion and Kudryashov's generalized quintuple-power nonlinearity," Results in Physics, **59**, 107589 (2024). https://doi.org/10.1016/j.rinp.2024.107589

[17] M. I. Khan, A. Farooq, K. S. Nisar, and N. A. Shah, "Unveiling new exact solutions of the unstable nonlinear Schrödinger equation using the improved modified Sardar sub-equation method," Results in Physics, **59**, 107593 (2024). https://doi.org/10.1016/j.rinp.2024.107593

[18] K. J. Wang, F. Shi, J. H. Liu, and J. Si, "Application of the extended F-expansion method for solving the fractional Gardner equation with conformable fractional derivative," Fractals, **30**(07), 2250139 (2022). https://doi.org/10.1142/S0218348X22501390

[19] S. Zhang, and T. Xia, "A generalized F-expansion method and new exact solutions of Konopelchenko–Dubrovsky equations," Applied Mathematics and Computation, **183**(2), 1190-1200 (2006). https://doi.org/10.1016/j.amc.2006.06.043

[20] W. M. Hasan, H. M. Ahmed, A. M. Ahmed, H. M. Rezk, and W. B. Rabie, "Exploring highly dispersive optical solitons and modulation instability in nonlinear Schrödinger equations with nonlocal self phase modulation and polarization dispersion," Scientific Reports, **15**(1), 27070 (2025). https://doi.org/10.1038/s41598-025-09710-8

[21] W. B. Rabie, and H. M. Ahmed, "Dynamical solitons and other solutions for nonlinear Biswas–Milovic equation with Kudryashov's law by improved modified extended tanh-function method," Optik, **245**, 167665 (2021). https://doi.org/10.1016/j.ijleo.2021.167665

[22] W. B. Rabie, A. R. Seadawy, and H. M. Ahmed, "Highly dispersive Optical solitons to the generalized third-order nonlinear Schrödinger dynamical equation with applications," Optik, **241**, 167109 (2021). https://doi.org/10.1016/j.ijleo.2021.167109

[23] K. A. Rashedi, M. Y. Almusawa, H. Almusawa, T. S. Alshammari, and A. Almarashi, "Applications of Riccati–Bernoulli and Bäcklund Methods to the Kuralay-II System in Nonlinear Sciences," Mathematics, **13**(1), 84 (2024). https://doi.org/10.3390/math13010084

[24] A. Biswas, A. Sonmezoglu, M. Ekici, A.Kh. Alzahrani, and M.R. Belic, "Cubic–quartic optical solitons with differential group delay for Kudryashov's model by extended trial function," Journal of Communications Technology and Electronics, **65**, 1384-1398 (2020). https://doi.org/10.1134/S1064226920120037

[25] W. B. Rabie, T. A. Khalil, N. Badra, H. M. Ahmed, M. Mirzazadeh, and M. S. Hashemi, "Soliton solutions and other solutions to the (4+1)-Dimensional Davey–Stewartson–Kadomtsev–Petviashvili equation using modified extended mapping method," Qualitative theory of dynamical systems, **36**(2), 87 (2024). https://doi.org/10.1007/s12346-023-00944-3

[26] W. M. Hasan, W. B. Rabie, A. M. Ahmed, H. M. Rezk, and H. M. Ahmed, "Construction of new travelling wave solutions and bifurcation analysis for the (2+1)-dimensional extended KP-BO equation utilizing the improved modified extended tanh-function method," International Journal of Computer Mathematics, **102**(12), 2214-2227 (2025). https://doi.org/10.1080/00207160.2025.2541068

[27] W. M. Hasan, H. M. Ahmed, A. M. Ahmed, H. M. Rezk, and W. B. Rabie, "Novel Soliton and Periodic Wave Solutions of the (3+1)-Dimensional Shallow Water Wave Equation with Bifurcation Analysis," Scientific Reports, **15**(1), 36490 (2025). https://doi.org/10.1038/s41598-025-21052-z

[28] Q. Cai, K. Tan, J. Li. Bifurcations and exact traveling wave solutions for the regularized Schamel equation. Open Mathematics, 19(1) (2021): 1699-1712. https://doi.org/10.1515/math-2021-0136

[29] A. A. Elmandouh, and M. E. Elbrolosy, "New traveling wave solutions for Gilson-Pickering equation in plasma via bifurcation analysis and direct method," Mathematical Methods in the Applied Sciences, 1-19 (2022). https://doi.org/10.1002/mma.8506

[30] W. Zhu, Y. Xia, and Y. Bai, "Traveling wave solutions of the complex Ginzburg-Landau equation with Kerr law nonlinearity," Applied Mathematics and Computation, **382**, 125342 (2020). https://doi.org/10.1016/j.amc.2020.125342

ТОЧНІ БІЖУЧІ ХВИЛІ ТА БІФУРКАЦІЙНА СТРУКТУРА ЗВ'ЯЗАНОЇ НЕЛІНІЙНОЇ СИСТЕМИ ШРЕДІНГЕРА ТИПУ КУДРЯШОВА ЗА ДОПОМОГОЮ МОДИФІКОВАНОГО МЕТОДУ РОЗШИРЕНОГО ВІДОБРАЖЕННЯ

Вафі М. Хасан[1,2], Хамді М. Ахмед[3], Ахмед М. Ахмед[1], Хайтам М. Резк[1], Вафаа Б. Рабі[4,5]

[1]*Кафедра математики, Факультет природничих наук, Університет Аль-Азхар, Каїр, Єгипет*

[2]*Кафедра фундаментальних наук, Факультет інженерних технологій, Технологічний університет Ель-Северді, Каїр, Єгипет*

[3]*Кафедра фізики та інженерної математики, Вищий інженерний інститут, Академія Ель-Шорук, Каїр, Єгипет*

[4]*Кафедра математики, Факультет наук, Луксорський університет, Тайба, Луксор, Єгипет*

[5]*Луксорський національний університет, Факультет обчислювальної техніки, інформаційних технологій та штучного інтелекту, Луксор, Єгипет*

У цьому дослідженні отримано точні розв'язки біжучої хвилі та проведено біфуркаційний аналіз для зв'язаного (1+1)-вимірного рівняння Кудряшова. Ця система нелінійних рівнянь типу Шредінгера моделює одночасне поширення оптичних імпульсів у двопроменепроменевому волокні, включаючи критичні ефекти вищого порядку, такі як кубічно-квартикова дисперсія та нелінійності, для підвищення фізичної точності. Застосовуючи модифікований метод розширеного відображення (MEMM), зв'язані диференціальні рівняння з частинними похідними систематично зводяться до керованого звичайного диференціального рівняння. Це зведення дозволяє побудувати широкий спектр точних розв'язків, таких як яскраві та темні солітони, періодичні хвилі, періодичні сингулярні розв'язки, а також сингулярні солітони, на додаток до гіперболічних, експоненціальних, раціональних та еліптичних функцій Вейєрштрасса. Ключовим компонентом роботи є детальний біфуркаційний аналіз результуючої плоскої динамічної системи. Цей аналіз визначає порогові значення критичних параметрів та класифікує всі можливі якісні поведінки хвильових рішень, відображаючи області існування для різних типів рішень. Фізичні наслідки як отриманих рішень, так і біфуркаційної структури обговорюються в контексті нелінійної оптики, зокрема для динаміки імпульсів та стабільності в системах оптичного зв'язку з подвійною поляризацією. Результати демонструють ефективність MEMM та надають нові знання, що сприяють розумінню та проектуванню передових оптичних хвилеводів.

Ключові слова: *нелінійні рівняння Шредінгера; двопроменепроменеві оптичні волокна; дисперсія вищого порядку; модифікований метод розширеного відображення (MEMM); точні рішення біжучої хвилі; біфуркаційний аналіз*